Angular dependence of X-ray absorption spectra

1990 J. Phys.: Condens. Matter 2 701

(http://iopscience.iop.org/0953-8984/2/3/018)

J. Phys.: Condens. Matter 2 (1990) 701–738. Printed in the UK

Angular dependence of x-ray absorption spectra

Christian Brouder
Laboratoire de Physique du Solide, Université de Nancy I, BP 239,
F-54506 Vandoeuvre-lès-Nancy Cédex, France

Received 13 March 1989, in final form 8 June 1989

Abstract. A detailed account of the dependence of x-ray absorption spectra (XAS) on polarisation and light beam directions is given. Anisotropic XAS measured on single crystals, layered compounds, polymers and oriented powders are tabulated. The x-ray absorption cross section by non-magnetic samples is derived, including electric dipole and quadrupole contributions. Orders of magnitude are found for magnetic dipole and electric dipole–octupole terms. Using a spherical tensor expansion of the absorption cross section, simple analytical formulae are given for the angular dependence of the electric dipole and quadrupole contributions to XAS for all crystal point groups. These formulae are valid down to the edge and include many-body effects. They are applied to two experimental examples, the iron K-edge in haematite and the copper K-edge in $CuCl_4^{2-}$. For the latter case, spherical tensor components are interpreted in terms of molecular orbitals. The influence of unpolarised and circularly polarised x-rays is discussed, as well as various experimental problems met in angle-resolved XAS. In an appendix, the quadrupole contribution to angular XAS is derived within the multiple-scattering formalism, along with closed expressions for the dipole and quadrupole spherical tensor components.

1. Introduction

The polarisation dependence of the x-ray absorption spectra (XAS) was considered early in the history of spectroscopy. In 1932, Kronig [1] noted that there should be a difference between the spectra of single crystals obtained from polarised and unpolarised x-rays. Then, Cooksey and Stephenson suggested that the spectra depend on the polarisation direction relative to the crystal axes [2]. An experimental observation of this effect was attempted in 1933 on a KBr single crystal [3] with dubious results because of a very high noise level and the cubic structure of the sample.

From 1948 to 1951, Hellwege published a series of papers [4–6] concerning a related problem: the angular dependence of the electric dipole, magnetic dipole and electric quadrupole contributions to the emission of light by crystals, based on quantum theory. In particular, he showed that the electric dipole transition probability is isotropic in a cubic crystal. In spite of this, quite a few experiments were carried out subsequently to investigate the angular dependence of the x-ray absorption spectra of cubic single crystals (KCl, NaCl [7], Ge [8, 9], Cu [10]). The situation was more or less settled in 1963 by Alexander *et al* [11], who made it clear for the XAS community that substantial information on the angular dependence of the x-ray absorption spectra could be obtained from group theory.

0953-8984/90/030701 + 38 $03.50

Throughout this paper, the phrases 'angular XAS', 'anisotropic XAS' or 'angle-resolved XAS' are used instead of the more common 'polarised XAS' because the latter name conveys the idea that polarised light is necessary for such experiments. As shown in §7.1, anisotropic XAS can be obtained with completely unpolarised x-rays.

Within the last few years, the number of angle-resolved XAS measurements has increased considerably, but the angular variation of x-ray absorption spectra for non-cubic samples is not always fully exploited. This paper gives a comprehensive account of the angular dependence of XAS for all the crystal symmetry groups. An XAS mainly reflects the dipole transitions from the initial state. However, some pre-edge structures of transition-metal compounds have been attributed to quadrupole transitions (see, e.g., [12–16]). The angular dependence of both dipole and quadrupole contributions to XAS is given. As noted first by Brümmer *et al* [17], this permits a clear discrimination between dipole and quadrupole transitions.

The present article is a theoretical investigation addressed to experimentalists and the mathematical demonstrations are relegated to appendices at the end of the paper. Although an attempt is made to show for specific examples how physical information can be drawn from the spectra, the main purpose of this paper is to give ready-to-use formulae with which experiments can be planned to obtain all the available data.

The conceptual basis of this paper is a spherical tensor expansion of the absorption cross section. This expansion is interesting from experimental and theoretical points of view. On the one hand, a large number of experimental spectra for various polarisation directions can be summarised in a few spectra (the components of the expansion) that contain all the angular dependence data; on the other hand, the theoretical absorption cross section for all the polarisation directions can be calculated with only one run of a multiple-scattering program. Moreover, since the tensor expansion is a consequence of the symmetry of the sample, it is rigorous on the whole energy range. Thus, a correct angular dependence is an indication that spurious effects (normalisation, thickness effects, pin-holes) [18, 19] are negligible or have been properly taken into account.

The first part of this paper is a self-contained derivation of the x-ray absorption cross section of a linearly polarised x-ray beam, discussing the approximations that lead to the formula commonly used. Then, the angular dependence of the electric dipole and quadrupole terms is discussed. The paper concludes with a discussion of the physical advantage of the additional selectivity offered by linearly polarised x-ray absorption spectra: it enables an unambiguous assessment of the quadrupolar nature of some pre-edge peaks to be established, it yields information concerning the angular part of the photoelectron wavefunction and it can be used to measure the orientation of a crystal or the degree of polarisation of x-rays. In appendices, the formulae given in the text are proved and the tensor components of the electric dipole and quadrupole absorptions are calculated by the multiple-scattering formalism.

2. Angle-resolved absorption spectra

Angle-resolved x-ray absorption spectroscopy has been used to study single crystals (table 1), layered compounds (table 2), polymers (table 3), oriented powders (table 4) and surfaces. Most surface extended x-ray absorption fine structure (SEXAFS) experiments show polarisation-dependent data, but no reference to any particular system is made here since the subject was reviewed recently by Stöhr [20]. However, x-ray absorption studies of polymers are included, although they could be considered as

Table 1. Angle-resolved absorption spectra of single crystals

Edge	Crystal	Reference
Ba K-edge	$YBa_2Cu_3O_y$	[78, 188]
Br K-edge	KBr	[3]
	$KBrO_3$	[40]
C K-edge	Graphite	[105, 106]
Cd K-edge	Cd	[53, 71, 73, 92, 189]
Cl K-edge	NaCl	[7]
	KCl	[7]
	$KClO_3$	[185, 186, 222]
Co K-edge	$Co^{III}(NH_3)_6(ClO_4)_2Cl$. KCl	[190]
Cr K-edge	Cr^{IV}(5,10,15,20-tetra-*p*-tolylporphyrin)O	[140, 180]
	Cr^{V}(5,10,15,20-tetra-*p*-tolylporphyrin)N	[140]
Cu K-edge	Cu	[10, 191]
	(creatinium)$_2CuCl_4$	[82, 130, 131, 134, 141, 153]
	$CuCl_2 . 2H_2O$	[131, 132]
	Cu(1-methylimidazole)$_2Cl_2$	[153]
	Cu(1,2-dimethylimidazole)$_2Cl_2$	[153]
	Plastocyanin	[69, 82, 138, 139, 220]
	Cu(2-methylpyridine)$_2Cl_2$	[139, 141, 153]
	Cu(imidazole)$_2Cl_2$	[139, 141, 153]
	Cu(imidazole)$_4$	[82]
	Cu(imidazole)$_4 . 2NO_3$	[141, 153]
	Cu(1,3,5-trimethylpyrazole)$_2BF_4$	[153]
	Cu(1,4,5-trimethylimidazole)$_4 . 2ClO_4$	[141, 153]
	Cu^{II}cyclam-$(SC_6F_5)_2$	[138]
	$YBa_2Cu_3O_y$	[77, 142, 188, 192]
	$ErBa_2Cu_3O_y$	[224]
	La_2CuO_{4-y}	[143]
	Cs_2CuCl_4	[82]
Cu L_{III}-edge	$YBa_2Cu_3O_{7-\delta}$	[144, 145, 193]
Fe K-edge	Fe	[129, 194]
	$FeCO_3$	[129, 194, 221]
	α-Fe_2O_3	[17, 129, 163, 194, 221]
	FeS_2	[129]
	biotite	[76]
	chlorite	[76]
	carboxymyoglobin	[173, 174]
	Fe porphyrins	[195]
	$Na_2[Fe(CN)_5NO] . 2H_2O$	[75]
	Azotobacter vinelandii ferredoxin I	[196]
Ga K-edge	Ga	[47, 49, 53, 155, 156, 197–199]
	GaS	[80, 83, 200]
	$GaS_{0.6}Se_{0.4}$	[200]
	GaSe	[83, 200]
Ge K-edge	Ge	[8, 9, 11, 194]
	GeS	[58]
I K-edge	$LiIO_3$	[42]
In L_{III}-edge	InSe	[83]
Mo K-edge	$MoO_2S_2(NH_4)_2$	[137]
	Nitrogenase	[72]
	$(Et_4N)_3$-$[Fe_6Mo_2S_8(SEt)_9]$	[72]
	$(Ph_4P)_2$-$[Cl_2FeS_2MoS_2FeCl_2]$	[72]
Mo $L_{II,III}$-edge	$[Et_4N]$-$[MoOCl_4(H_2O)]$	[201]
Nb K-edge	$LiNbO_3$	[44, 45]
Nd L_{III}-edge	Nd-exchanged Na-β''-alumina	[202]

continued over

Table 1—*cont.*

Edge	Crystal	Reference
Ni K-edge	$K_2Ni(CN_4)H_2O$	[136]
	$NiPc(SbF_6)_{0.5}$	[227]
O K-edge	$Bi_2Sr_2CaCu_2O_8$	[110, 133]
P K-edge	black phosphorus	[203, 204]
P $L_{II,III}$-edge	black phosphorus	[205]
Pt $L_{I,II,III}$-edge	K_2PtCl_4	[41]
Pt L_{III}-edge	$Pt^{I}(2,2'bipyridine)_2NO_3 . 2H_2O$	[206]
	$Pt^{II}(2,2'bipyridine)_2Pt(CN)_4 . nH_2O$	[206]
S K-edge	$CuSO_4 . 5H_2O$	[185]
	$MgS_2O_3 . 6H_2O$	[185]
	$K_2S_2O_6$	[185, 186]
	GaS	[80]
S $L_{II,III}$-edge	CdS	[207]
U $L_{I,III}$-edge	$RbUO_2(NO_3)_3$	[39]
V K-edge	V_2O_5	[116]
	$V_2O_5 . 1.6H_2O$	[70]
	$VO(C_5H_7O_2)_2$	[38]
Y K-edge	$YBa_2Cu_3O_y$	[77, 188]
Zn K-edge	Zn	[57, 208, 209]
	ZnF_2	[59]

SEXAFS experiments, because they do not always require the specific conditions of surface science (e.g. ultra-high vacuum). These tables are not exhaustive and are focused on the physics literature but they show that angular x-ray absorption spectroscopy was decisive for a very broad range of applications (solid-state, surfaces, minerals, organic and inorganic chemistry, biology). Usually, the anisotropy of XAS is particularly marked at the K-edge, because the p-waves attained in the final state are highly directional.

3. Derivation of the x-ray absorption cross section

In this section a derivation of the absorption cross section including the electric dipole, electric quadrupole and magnetic dipole terms is presented. In the specific case of the x-ray range, the order of magnitude of the quadratic term (A^2), of the magnetic dipole contribution and of the interference between electric dipole and octupole matrix elements are discussed. The calculations of this section will be carried out within a one-electron framework but they can be adapted to the many-body case since the initial and final states are not specified.

3.1. General expression of the transition amplitude

In non-relativistic quantum theory, a particle with charge q, mass m, gyromagnetic factor g ($\simeq 2$ for the electron) and spin s in a potential $V(\boldsymbol{r})$, submitted to an external electromagnetic field $(\Phi(\boldsymbol{r}, t), \boldsymbol{A}(\boldsymbol{r}, t))$ is described by the Hamiltonian (in SI units)

$$H = (1/2m)[-i\hbar\boldsymbol{\nabla} - q\boldsymbol{A}]^2 + V(\boldsymbol{r}) + q\Phi - (gq/2m)\boldsymbol{s}\cdot\boldsymbol{B} \tag{3.1}$$

$$H = H_0 + (i\hbar q/m)\boldsymbol{A}\cdot\boldsymbol{\nabla} + (i\hbar q/2m)(\boldsymbol{\nabla}\cdot\boldsymbol{A}) + (q^2/2m)A^2 + q\Phi - (gq/2m)\boldsymbol{s}\cdot\boldsymbol{B} \tag{3.2}$$

Table 2. Angle-resolved absorption spectra of Langmuir–Blodgett films (L-B), layered or intercalation compounds.

Edge	Sample	Reference
As K-edge	AsF_5 in graphite	[210]
Br K-edge	Br_2 in graphite	[63, 64, 84]
C K-edge	L-B of cadmium arachidate	[107, 111, 211, 212]
	L-B of cadmium tetradecylfumarate	[212]
	L-B of cadmium octadecylfumarate	[212]
	L-B of calcium arachidate	[107, 111, 212]
	L-B of arachidic acid	[111, 212]
	L-B of polypyrrole	[213]
Ca $L_{II,III}$-edge	CaF_2/Si(111)	[214]
Cl K-edge	ICl in graphite	[85–87]
Co K-edge	$CoSi_2$/Si(111)	[94]
Cu K-edge	L-B of Cu-phthalocyanine	[215]
	Mitochondrial cytochrome oxidase	[81, 91]
	$Cu_{0.5}NbS_2$	[93]
I $L_{I,III}$-edge	ICl in graphite	[85–88]
F K-edge	CaF_2/Si(111)	[214]
Fe K-edge	Mitochondrial cytochrome oxidase	[81, 91]
K K-edge	K in graphite	[89, 104, 113, 114, 216]
Mn K-edge	photosynthetic water-splitting enzyme	[81]
Mo L_{III}-edge	MoS_2	[223]
Rb K-edge	Rb in graphite	[89, 90, 113]
S K-edge	MoS_2	[223]
	TiS_2	[223]
Se K-edge	2H–WSe_2	[18]
	$MoSe_2$	[223]
	$NbSe_2$	[223]
	$TaSe_2$	[223]
	L-B of merocyanin dye	[61]
Ta L_{III}-edge	1T–TaS_2	[135]
Ti K-edge	TiS_2	[103, 223]
W L_{III}-edge	2H–WSe_2	[18]
Zn K-edge	Mitochondrial cytochrome oxidase	[81]

Table 3. Angle-resolved absorption spectra of polymers.

Edge	Sample	Reference
Br K-edge	Br-doped trans-polyacetylene	[21, 62, 65, 67, 68, 74, 177, 178]
C K-edge	Polyethylene	[181, 212]
	Poly(di-*n*-hexylsilane)	[66]
	Poly-3-alkylthiophene	[108, 146, 147, 217]
	Polyacrylonitrile	[148]
I L_I-edge	I-doped trans-polyacetylene	[62, 74, 176, 179]
N K-edge	Polyacrylonitrile	[148]
S $L_{II,III}$-edge	Poly-3-methylthiophene	[108, 146]
Se K-edge	$(TMTSeF)_2ReO_4$	[117]
Si K-edge	Poly(di-*n*-hexylsilane)	[66]

Table 4. Angle-resolved absorption spectra of oriented powders.

Edge	Sample	Reference
Cu K-edge	$La_{1.85}Ba_{0.15}CuO_4$	[112]
	La_2CuO_4	[226]
	$YBa_2Cu_3O_y$	[79, 218, 219, 226]
	$La_{2-x}Sr_xCuO_4$	[218, 226]
	$Bi_2Sr_{1.75}Ca_{1.25}Cu_2O_{8+x}$	[219]
	$La_{1.85}Sr_{0.15}Cu_2O_4$	[219]
	$Tl_2Ba_2CaCu_2O_x$	[219]
	$Tl_2Ba_2Ca_2Cu_3O_x$	[219]
Y K-edge	$YBa_2Cu_3O_7$	[79, 218]

where

$$H_0 = -(\hbar^2/2m)\nabla^2 + V(\boldsymbol{r}). \tag{3.3}$$

If the exciting electromagnetic field is a plane wave expressed in the Coulomb gauge then $\Phi = 0$ and $(\nabla \cdot \boldsymbol{A}) = 0$ so that ∇ and $\boldsymbol{A}$ can be considered as commutating operators. The term $(q^2/2m)A^2$ is negligible for available x-ray sources. To show this, let $I(\omega)$ be the intensity of the impinging monochromatic x-rays. Since $I(\omega) = (1/2)\varepsilon_0 c A^2 \omega^2$, the ratio of the quadratic term over the linear term is

$$|q^2A^2/2m|/|\hbar q\boldsymbol{A}\cdot\nabla/m| \sim |qa_0A|/2\hbar = (\sqrt{I(\omega)}/\omega)a_0\sqrt{2\pi\alpha/\hbar} \tag{3.4}$$

where the electron momentum $|i\hbar\nabla\varphi|$ is approximated by $\hbar/a_0$ (a_0 is the Bohr radius). Oyanagi *et al* [21] report a typical flux of 10^8 photons per second at 9 keV with a 6 mm^2 beam spot (energy resolution = 1.1 eV), so that $I(\omega) \simeq 2.4 \times 10^{-2}$ W m^{-2} and $\omega \simeq 1.4 \times 10^{19}$ s^{-1}, which yields a ratio of the quadratic over the linear term of around 10^{-14}: the quadratic term is completely insignificant.

Therefore, what remains is

$$H = H_0 + (i\hbar q/m)\boldsymbol{A}\cdot\nabla - (gq/2m)\boldsymbol{s}\cdot\boldsymbol{B}. \tag{3.5}$$

The incident plane wave can be written

$$\boldsymbol{A}(\boldsymbol{r}, t) = A_0\hat{\varepsilon}\exp[i(\boldsymbol{k}\cdot\boldsymbol{r} - \omega t)] + A_0\hat{\varepsilon}^*\exp[-i(\boldsymbol{k}\cdot\boldsymbol{r} - \omega t)] \tag{3.6}$$

where $\hat{\varepsilon}$ is the polarisation vector, $\boldsymbol{k}$ the x-ray wavevector and $\sqrt{2}A_0$ the vector potential amplitude. According to time-dependent perturbation theory, the transition probability per unit time for a perturbation $W(t) = W\exp(-i\omega t) + W^*\exp(i\omega t)$ is [22]

$$w = (2\pi/\hbar)\sum_{\mathrm{f}} |\langle \mathrm{f}|W|\mathrm{i}\rangle|^2\delta(E_\mathrm{f} - E_\mathrm{i} - \hbar\omega). \tag{3.7}$$

In the case of a plane electromagnetic wave, since $\boldsymbol{B} = \nabla \times \boldsymbol{A}$,

$$w = (2\pi q^2|A_0|^2/\hbar m^2)\sum_{\mathrm{f}} |\langle \mathrm{f}|\exp[i(\boldsymbol{k}\cdot\boldsymbol{r})]\{\hbar\hat{\varepsilon}\cdot\nabla - (g/2)\boldsymbol{s}\cdot(\boldsymbol{k}\times\hat{\varepsilon})\}|\mathrm{i}\rangle|^2$$
$$\times\,\delta(E_\mathrm{f} - E_\mathrm{i} - \hbar\omega). \tag{3.8}$$

The absorption cross section $\sigma(\omega)$ is defined as the ratio of the rate at which energy is removed from the photon beam by the photoelectric effect ($w\hbar\omega$), divided by the rate

at which energy in the photon beam crosses a unit area perpendicular to its propagation direction:

$$I(\omega) = 2\varepsilon_0 c|A_0|^2\omega^2. \tag{3.9}$$

Therefore

$$\sigma(\omega) = (4\pi^2\hbar\alpha/m^2\omega)\sum_{\mathrm{f}}|\langle \mathrm{f}|\exp[\mathrm{i}(\boldsymbol{k}\cdot\boldsymbol{r})]\{\hbar\hat{\varepsilon}\cdot\boldsymbol{\nabla} - (g/2)\boldsymbol{s}\cdot(\boldsymbol{k}\times\hat{\varepsilon})\}|\mathrm{i}\rangle|^2$$
$$\times\,\delta(E_{\mathrm{f}} - E_{\mathrm{i}} - \hbar\omega). \tag{3.10}$$

If $|\mathrm{i}\rangle$ and $|\mathrm{f}\rangle$ are many-electron wavefunctions, a sum over electron coordinates and spins is implicitly assumed.

Since the mean radius of the 1s orbital of an atom with effective atomic number Z_{eff} is a_0/Z_{eff}, an accurate description of core-level absorption is given by the first few terms of the multipole expansion of $\exp[\mathrm{i}(\boldsymbol{k}\cdot\boldsymbol{r})]$.

To obtain a transition amplitude including the electric dipole, electric quadrupole and magnetic dipole contributions, $\exp[\mathrm{i}(\boldsymbol{k}\cdot\boldsymbol{r})]$ is expanded to first order:

$$\exp[\mathrm{i}(\boldsymbol{k}\cdot\boldsymbol{r})] \simeq 1 + \mathrm{i}\boldsymbol{k}\cdot\boldsymbol{r}. \tag{3.11}$$

Then, the velocity form for the electric dipole matrix elements is transformed into the more commonly used length form by using the equation of motion of $\boldsymbol{p}$ which is

$$\boldsymbol{p} = -\mathrm{i}\hbar\boldsymbol{\nabla} = (m/\mathrm{i}\hbar)[\boldsymbol{r}, H_0]. \tag{3.12}$$

Hence

$$\langle \mathrm{f}|\hbar\hat{\varepsilon}\cdot\boldsymbol{\nabla}|\mathrm{i}\rangle = -[m(E_{\mathrm{f}} - E_{\mathrm{i}})/\hbar]\langle \mathrm{f}|\hat{\varepsilon}\cdot\boldsymbol{r}|\mathrm{i}\rangle. \tag{3.13}$$

Note that the equivalence of the velocity and length forms of the electric dipole operator is valid only when the exact wavefunctions are known for $|\mathrm{i}\rangle$ and $|\mathrm{f}\rangle$. For approximate wavefunctions, they are usually different [23].

To obtain the standard quadrupole term, one uses the identity [24]

$$\hbar\boldsymbol{k}\cdot\boldsymbol{r}\,\hat{\varepsilon}\cdot\boldsymbol{\nabla} = (m/2\hbar)[\hat{\varepsilon}\cdot\boldsymbol{r}\,\boldsymbol{k}\cdot\boldsymbol{r}, H_0] + (\mathrm{i}/2)(\boldsymbol{k}\times\hat{\varepsilon})\cdot\boldsymbol{L} \tag{3.14}$$

where $\boldsymbol{L}$ is the angular momentum operator. Therefore, the transition amplitude becomes

$$-[m(E_{\mathrm{f}} - E_{\mathrm{i}})/\hbar]\langle \mathrm{f}|\hat{\varepsilon}\cdot\boldsymbol{r}|\mathrm{i}\rangle - \mathrm{i}[m(E_{\mathrm{f}} - E_{\mathrm{i}})/2\hbar]\langle \mathrm{f}|\hat{\varepsilon}\cdot\boldsymbol{r}\,\boldsymbol{k}\cdot\boldsymbol{r}|\mathrm{i}\rangle$$
$$-\,(1/2)\langle \mathrm{f}|(\boldsymbol{k}\times\hat{\varepsilon})\cdot(\boldsymbol{L} + g\boldsymbol{s})|\mathrm{i}\rangle \tag{3.15}$$

where the first, second and third terms are the electric dipole, electric quadrupole and magnetic dipole transition amplitudes respectively. In the emission spectra of oxygen and nitrogen, the magnetic dipole transitions give rise to lines observed in the spectra of some nebulae, called nebulium lines because they were thought to be due to a new element not discovered on Earth. The electric quadrupole transitions in the spectra of O^+ is the origin of the green line of the aurora and the night sky.

3.2. Magnetic dipole transitions in the x-ray range

A priori, the electric quadrupole and the magnetic dipole transition probabilities have the same order of magnitude: $(Z_{\mathrm{eff}}/137)^2$ times the electric dipole [23]. However, the magnetic dipole operator does not incorporate a radial variable, so that its matrix

elements vanish if the radial part of the initial and final states are orthogonal. For atomic spectroscopy, within an L–S coupling scheme, the one-electron magnetic dipole transition rules are $|\Delta j| \leqslant 1$, $\Delta l = 0$, $\Delta s = 0$ and $\Delta n = 0$ (identical principal quantum numbers). This means that magnetic dipole absorption occurs at low energy (typically in the microwave–optical range [25, 26]). Its occurrence at higher energy implicates an appreciable configuration interaction between the initial and final states, due to a departure from a pure L–S coupling [25, 27]. However, such a configuration interaction is negligible for core-level spectroscopies, because of the large energy difference between the initial and final states (typically 1 keV). This conclusion can be extended to the case of molecules. Since the core-level wavefunctions do not overlap the states of similar energy of the neighbouring atoms, the spatial part of the one-electron initial states can be taken as an eigen-state of angular momentum centred on the photoabsorbing atom: $\langle \boldsymbol{r}|\mathrm{i}\rangle = \langle \boldsymbol{r}|nlm\rangle$. Moreover, the states corresponding to all values of m are occupied. The final states $|\mathrm{f}\rangle$ of the molecule are orthogonal to $|nlm\rangle$ for all m. Therefore, $\langle \mathrm{f}|(\boldsymbol{k}\times\hat{\boldsymbol{\varepsilon}})\cdot\boldsymbol{L}|\mathrm{i}\rangle = (\boldsymbol{k}\times\hat{\boldsymbol{\varepsilon}})\cdot\langle \mathrm{f}|\boldsymbol{L}|nlm\rangle = 0$ because the components of $\boldsymbol{L}|nlm\rangle$ are linear combinations of $|nlm-1\rangle$, $|nlm\rangle$ and $|nlm+1\rangle$ which are all orthogonal to $|\mathrm{f}\rangle$. The spin contribution to the magnetic dipole transition vanishes for the same reason. Taking spin–orbit coupling into account does not change the conclusion.

In practical calculations, the Hamiltonians H_0 for the initial (core electron) and final (photoelectron) states are different, and the radial parts of the initial and final wavefunctions are not automatically orthogonal but the agreement with experiment is generally improved by imposing orthogonality [28, 29].

However, magnetic dipole transitions in the x-ray range are possible for heavy atoms because relativistic effects break the $\Delta n = 0$ selection rule [30, 31]. An estimate of the magnetic dipole term can be obtained from a ratio of the magnetic to electric dipole oscillator strengths. Since this ratio increases rapidly with Z [32], we shall take the case of hafnium ($Z = 72$). Edlabadkar and Mande have calculated magnetic dipole oscillator strengths of heavy atoms [32]. For hafnium, they find that the strength of the transition $\mathrm{K}\rightarrow \mathrm{O_I}$ is $f_K^{\mathrm{M}} \simeq 10^{-6}$ and that of $\mathrm{L_I}\rightarrow \mathrm{O_I}$ is $f_{L_\mathrm{I}}^{\mathrm{M}} \simeq 10^{-7}$. According to equation (18.46) of reference [25], oscillator strengths match smoothly to densities of oscillator strength so that, near the edge, $\mathrm{d}f_K^{\mathrm{M}}/\mathrm{d}E \simeq 10^{-7}\ \mathrm{Ryd}^{-1}$ and $\mathrm{d}f_{L_\mathrm{I}}^{\mathrm{M}}/\mathrm{d}E \simeq 10^{-8}\ \mathrm{Ryd}^{-1}$. From the absorption cross section across the hafnium K- and $\mathrm{L_I}$-edges [33] a jump of the electric dipole densities of oscillator strength across the edges $\mathrm{d}f_K^{\mathrm{E}}/\mathrm{d}E \simeq 5\times 10^{-4}\ \mathrm{Ryd}^{-1}$ and $\mathrm{d}f_{L_\mathrm{I}}^{\mathrm{E}}/\mathrm{d}E \simeq 10^{-3}\ \mathrm{Ryd}^{-1}$ is obtained. The ratio of the magnetic to electric dipole contributions to the absorption cross section at the hafnium K- and $\mathrm{L_I}$-edges is 2×10^{-4} and 10^{-5} respectively. This ratio is still smaller at the $\mathrm{L_{II}}$- and $\mathrm{L_{III}}$-edges. Therefore, even if relativistic effects are taken into account, the magnetic dipole contribution is negligible. This conclusion is not modified by many-body effects.

3.3. The dipole–octupole term

If the expansion of $\exp(\mathrm{i}\boldsymbol{k}\cdot\boldsymbol{r})$ is made up to the next order, the term $-(\boldsymbol{k}\cdot\boldsymbol{r})^2/2$ gives rise to an electric octupole contribution that interferes with the electric dipole transition amplitude. This is the dipole–octupole term discussed in references [34] and [35]. When polarisation is linear, the magnetic quadrupole term is purely complex and gives no interference. *A priori*, dipole–octupole transitions have the same order of magnitude as electric quadrupole transitions. They have not been taken into account here because the calculation of the dipole–octupole term for germanium [35] shows that it is at least three times smaller than the quadrupole term. Moreover, a large part of it is of the form

$|\langle f|\hat{\varepsilon}\cdot\boldsymbol{r}|i\rangle|^2$ and can be included in the electric dipole term (this is partly due to the fact that the expansion (3.11) of $\exp(i\boldsymbol{k}\cdot\boldsymbol{r})$ does not correspond to the rigorous multipole expansion [36]). Finally, the dipole–octupole term is negligible when the dipole term is small and the analysis, for example, of the p/d character of the pre-peak structures at the K-edge of transition metals can be done safely with dipole and quadrupole contributions only. However, dipole–octupole transitions may deserve further investigation.

3.4. Final form of the absorption cross section in the x-ray range

According to the foregoing considerations, only electric dipole and electric quadrupole terms are expected to contribute to x-ray absorption spectra significantly. The order of magnitude of the quadrupole term will be discussed in § 5. To reach the final form of the absorption cross section, the discussion must be restricted to non-magnetic samples. Then the initial- and final-state wavefunctions can always be chosen real (§ 18 of reference [22]). Since the present analysis is limited to linear polarisation (except in § 7.1), the matrix elements $\langle f|\hat{\varepsilon}\cdot\boldsymbol{r}|i\rangle$ and $\langle f|\hat{\varepsilon}\cdot\boldsymbol{r}\boldsymbol{k}\cdot\boldsymbol{r}|i\rangle$ are real and the electric dipole and quadrupole transition amplitudes do not interfere. Thus, the absorption cross section that will be the basis of the rest of the paper is:

$$\sigma(\omega) = 4\pi^2\alpha\hbar\omega \sum_{if} \{|\langle f|\hat{\varepsilon}\cdot\boldsymbol{r}|i\rangle|^2 + (1/4)|\langle f|\hat{\varepsilon}\cdot\boldsymbol{r}\boldsymbol{k}\cdot\boldsymbol{r}|i\rangle|^2\}\delta(E_f - E_i - \hbar\omega). \tag{3.16}$$

The sum over the initial states $|i\rangle$ is due to the fact that, in inner-shell absorption and within a one-electron framework, all the states with energy E_i are occupied. In a many-body description there is no sum over i since the initial state describes all the electrons.

4. The electric dipole term

As shown in appendix 1, the polarisation-dependent absorption cross section has the same structure as the dielectric constant of anisotropic media. In optics, the anisotropy of the absorption coefficient is called pleochroism, because if white light is incident upon the crystal, the crystal will in general appear coloured, and the colour will depend on the polarisation direction of the incident light [37]. This phenomenon is related to the polarised anomalous scattering of x-rays [38–45] in which the refractive index depends on the direction of the electric vector: this is the birefringence of crystals for x-rays.

Firstly, the dependence of the single-scattering EXAFS on the angle between the interatomic bond and the polarisation vector is given, then the angular dependence of the full spectra is presented as a function of polarisation direction and symmetry of the crystal.

4.1. Single-scattering region (EXAFS)

The early theories of the angular dependence of x-ray absorption spectra were usually limited to the high-energy region [46–56]. The most famous of these theories [55] shows that the contribution of each neighbour for a K-edge is weighted by a factor $\cos^2\alpha$, where α is the angle between the polarisation and the neighbour directions. This angular

dependence was employed to analyse most of the experimental works. It has been used to find the neighbour distances in various directions since, for a K-edge, the directionality of the p components of the final state allows, in favourable cases, a selective detection of the neighbours in each direction [18, 21, 57–94] (see also [20] for a review of the SEXAFS work). For an L_{II}- or L_{III}-edge, the angular dependence is complicated by the presence of two final state components ($l = 0$ and $l = 2$) [18] which, if neglected, leads to significant errors in the bond length and geometry derived from angular spectra [95].

Recently, it was shown that a curved-wave description of the problem gives an addition term in $\sin^2 \alpha$ for a K-edge [96–99]. The relevance of this term to SEXAFS experiments has been demonstrated for O(2 × 1)/Cu(110) [99]. The polarised curved-wave EXAFS formula for an L_{II}- or L_{III}-edge is the sum of an isotropic term and an angle-dependent term weighted by the Legendre polynomial $(3\cos^2 \alpha - 1)/2$ [98]. Further detail concerning the angular dependence of the EXAFS region is not given here since it is now well known and, for single crystals, the structural information it yields can often be obtained by other techniques. The specific advantage of angle-resolved XAS is emphasised in the near-edge region where it gives detailed information on the electronic structure of the sample.

4.2. *Multiple-scattering (near-edge) region*

As shown in appendix 1, the dipole absorption cross section can be written on the whole energy range

$$\sigma^{\mathrm{D}}(\hat{\varepsilon}) = \sigma^{\mathrm{D}}(0,0) - \sqrt{8\pi/5} \sum_{m=-2}^{2} Y_2^{m*}(\hat{\varepsilon})\sigma^{\mathrm{D}}(2,m). \tag{4.1}$$

The first term is the isotropic absorption cross section (i.e. measured on powders), the second term describes the angular dependence of the spectra. The second term does not intervene in powder spectra because its average over angles is zero ($\int \mathrm{d}\Omega_\varepsilon Y_l^{m*}(\hat{\varepsilon}) = 0$ for $l \neq 0$). The tensor components $\sigma^{\mathrm{D}}(l,m)$ are generally complex numbers, that will be written $\sigma^{\mathrm{D}}(l,m) = \sigma^{\mathrm{Dr}}(l,m) + \mathrm{i}\sigma^{\mathrm{Di}}(l,m)$. Since $\sigma^{\mathrm{D}}(\hat{\varepsilon})$ is real, $\sigma^{\mathrm{D}}(l,m)$ satisfies the relation $\sigma^{\mathrm{D}}(l,-m) = (-1)^m[\sigma^{\mathrm{D}}(l,m)]^*$ (so that $\sigma^{\mathrm{D}}(l,0)$ is real). The parameters $\sigma^{\mathrm{D}}(l,m)$ are called tensor components because they transform under rotation like the spherical harmonics Y_l^m. According to the considerations developed in appendix 1, the symmetries of the molecule or crystal restrict the possible values of $\sigma^{\mathrm{D}}(2,m)$.

The following list gives the angular dependence of the dipole contribution to the x-ray absorption for all crystal point-symmetry groups. For completeness, the C_∞ symmetry group is also included because it is encountered in many samples, such as textured powders or crystals grown with only one axis along a specific direction, the others being random. In an orthonormal reference frame bound to the crystal the polarisation vector is written

$$\hat{\varepsilon} = \begin{pmatrix} \sin\theta\cos\varphi \\ \sin\theta\sin\varphi \\ \cos\theta \end{pmatrix}. \tag{4.2}$$

The orthonormal axes are chosen according to the *International Tables for X-ray Crystallography* [100] when the latter are orthonormal. The z axis is always that of the *Tables*. For trigonal or hexagonal symmetries, the x axis is taken parallel to the x axis of the *Tables*. When reporting experimental spectra, the axes chosen must be given explicitly.

Table 5. Point groups corresponding to each angular dependence of dipolar absorption.

Angular dependence	Point groups
Isotropy (i)	O_h (m3m), T_d ($\bar{4}$3m), O (432), T_h (m3), T (23)
Dichroism (ii)	$D_{\infty h}$(∞/mm), $C_{\infty v}$ (∞m), D_{6h} (6/mmm), D_{3h} ($\bar{6}$m2), C_{6v} (6mm), D_6 (622), C_{6h}(6/m), C_{3h} ($\bar{6}$), C_6 (6), D_{3d} ($\bar{3}$m), C_{3v} (3m), D_3 (32), S_6 ($\bar{3}$), C_3 (3), D_{4h} (4/mmm), D_{2d} ($\bar{4}$2m), C_{4v} (4mm), D_4 (422), C_{4h} (4/m), S_4 ($\bar{4}$), C_4 (4)
Trichroism (iii*a*)	D_2 (222), C_{2v} (mm2), D_{2h} (mmm)
Trichroism (iii*b*)	C_2 (2), C_s (m), C_{2h} (2/m)
Trichroism (iii*c*)	C_1 (1), C_i ($\bar{1}$)

As explained in appendix 1, it is the full point group of the crystal and not the local point group of the photoabsorber that rules the angular dependence (but see § A1.3 for the case of molecular crystals). The point groups are given with their Schoenflies and short international symbols. There are five classes of angular dependence. The point groups corresponding to each class are listed in table 5.

(i) Isotropy. For cubic symmetries $\sigma^D(2, m) = 0$ for all m and the absorption cross section due to the dipole transition is isotropic [4, 5, 11, 52]

$$\sigma^D(\hat{\varepsilon}) = \sigma^D(0, 0). \tag{4.3}$$

(ii) Dichroism. If there is a rotation axis of order greater than two then $\sigma^D(2, m) = 0$ for $m \neq 0$ and we obtain the simple formula

$$\sigma^D(\hat{\varepsilon}) = \sigma^D(0, 0) - (1/\sqrt{2})(3\cos^2\theta - 1)\sigma^D(2, 0) \tag{4.4}$$

where θ is the angle between the rotation axis and the polarisation vector.

This formula, which is often written as $\sigma(\hat{\varepsilon}) = \sigma_\parallel \sin^2\theta + \sigma_\perp \cos^2\theta$, has been known since the late sixties [18, 52, 101] and is valid over the whole energy range (from the edge to the high-energy region), like the other formulae of this section. It was checked experimentally in a number of cases [18, 44, 65, 72, 81, 91, 102–111, 226]. Note that formula (4.4) is also valid for cylindrically oriented powders and is the basis of the magic-angle measurements that give isotropic x-ray absorption spectra from oriented powders [112]. It should also be noticed that, at the energies where $\sigma^D(2, 0) = 0$, the spectrum is independent of polarisation direction. This is a good way to check spectrum normalisation: the spectra for all θ must cross at the same point. This behaviour can be observed in some published spectra [70, 74, 81, 112–114, 143].

(iii) Trichroism. Trichroism designates the case when all the eigenvalues of the absorption cross-section Cartesian tensor are different. An analysis of the symmetries of the absorption tensor show that there are three classes of trichroism.

(iii*a*) For the simplest class of trichroism one finds that $\sigma^D(2, 1) = \sigma^D(2, -1) = 0$ and $\sigma^D(2, 2) = \sigma^D(2, -2)$ so that

$$\sigma^D(\hat{\varepsilon}) = \sigma^D(0, 0) - \sqrt{3}\sin^2\theta\cos 2\varphi\,\sigma^{Dr}(2, 2) - (1/\sqrt{2})(3\cos^2\theta - 1)\sigma^D(2, 0) \tag{4.5}$$

and there are three independent parameters (i.e. at least three independent measurements have to be carried out).

(iii*b*) For the intermediate class of trichroism one has only $\sigma^D(2, 1) = \sigma^D(2, -1) = 0$ and

$$\sigma^D(\hat{\varepsilon}) = \sigma^D(0, 0) - \sqrt{3}\sin^2\theta[\cos 2\varphi\sigma^{Dr}(2, 2) + \sin 2\varphi\sigma^{Di}(2, 2)] - (1/\sqrt{2})(3\cos^2\theta - 1)\sigma^D(2, 0). \quad (4.6)$$

There are four independent parameters.

(iii*c*) The most complicated angular dependence is found for the lowest symmetries. In that case, one has

$$\sigma^D(\hat{\varepsilon}) = \sigma^D(0, 0) - \sqrt{3}\sin^2\theta[\cos 2\varphi\sigma^{Dr}(2, 2) + \sin 2\varphi\sigma^{Di}(2, 2)] + 2\sqrt{3}\sin\theta\cos\theta[\cos\varphi\sigma^{Dr}(2, 1) + \sin\varphi\sigma^{Di}(2, 1)] - (1/\sqrt{2})(3\cos^2\theta - 1)\sigma^D(2, 0) \quad (4.7)$$

with six independent tensor components to determine. A similar expression for the general case was given in reference [101].

In the cases of trichroism (iii*a*)–(iii*c*), the absorption cross section is polar- *and* azimuthal-angle dependent. This azimuthal angular dependence has already been investigated for a K-edge [52, 115]. The present analysis is valid for any edge and more clearly shows the number of independent parameters involved in linear polarisation experiments. The azimuthal dependence was observed in single crystals [69, 82, 116], polymers [66, 117], Langmuir–Blodgett films [61] and in SEXAFS experiments (e.g. (2×1)O on Cu(110) [62] and (2×1)O on Ni(110) [118]).

5. The electric quadrupole term

In atomic spectroscopy, the quantum theory of electric quadrupole transitions was elaborated by Rubinowicz and Blaton during the early thirties [119, 120]. The case of crystalline materials was investigated by Hellwege [4–6]. Electric quadrupole sum rules were developed by Rosenthal *et al* [121].

In 1966, Wagenfeld [34] showed that electric quadrupole transitions were the source of an angular dependence of the Borrmann effect, and that the electric quadrupole contribution to the absorption cross section could be measured from this angular dependence. He published with collaborators [35, 122, 123] a calculation of the intensity of the electric quadrupole absorption based on hydrogen-like wavefunctions, finding good agreement with experimental data for silicon and germanium. The quadrupole contribution obtained is usually a few per cent of the electric dipole contribution and increases with Z^2. This was confirmed by more recent calculations [124, 125, 130, 132]. It is larger at high energy and when the overlap of the initial- and final-state wavefunctions is substantial [126, 127].

Therefore, electric quadrupole transitions are well within the scope of our experimental capabilities, and their study can yield considerable information concerning the electronic structure of physical systems.

5.1. Angular dependence

This section presents the general formulae giving the angular dependence of the electric quadrupole absorption as a function of the point symmetry group of the crystal. The

general coordinates for the wavevector and the polarisation vector are

$$\hat{\varepsilon} = \begin{pmatrix} \sin\theta\cos\varphi \\ \sin\theta\sin\varphi \\ \cos\theta \end{pmatrix} \qquad \hat{k} = \begin{pmatrix} \cos\theta\cos\varphi\cos\psi - \sin\varphi\sin\psi \\ \cos\theta\sin\varphi\cos\psi + \cos\varphi\sin\psi \\ -\sin\theta\cos\psi \end{pmatrix}. \tag{5.1}$$

The angle ψ specifies the direction of the wavevector $\boldsymbol{k}$ in the plane perpendicular to $\hat{\varepsilon}$. Since the quadrupole cross section (A6) is symmetric in $\hat{k}$ and $\hat{\varepsilon}$, it is possible to interchange the definitions of $\hat{k}$ and $\hat{\varepsilon}$ without changing anything in the final formulae. The coordinates are chosen to take full advantage of the crystalline symmetries. The orthonormal axes are chosen as in § 4.2.

(i) For the cubic point groups O_h (m3m), T_d ($\bar{4}$3m), O (432), T_h (m3) and T (23), the symmetry average yields $\sigma^{Qr}(4,4) = \sigma^{Qr}(4,-4) = \sqrt{5/14}\sigma^{Q}(4,0)$, the other non-isotropic terms are zero and the quadrupole absorption cross section is

$$\begin{aligned}\sigma^{Q}(\hat{\varepsilon},\hat{k}) = \sigma^{Q}(0,0) &+ (1/\sqrt{14})[35\sin^2\theta\cos^2\theta\cos^2\psi + 5\sin^2\theta\sin^2\psi - 4 \\ &+ 5\sin^2\theta(\cos^2\theta\cos^2\psi\cos 4\varphi - \sin^2\psi\cos 4\varphi \\ &- 2\cos\theta\sin\psi\cos\psi\sin 4\varphi)]\sigma^{Q}(4,0).\end{aligned} \tag{5.2}$$

(ii) For the groups $D_{\infty h}(\infty/mm)$, $C_{\infty v}(\infty m)$, $D_{6h}(6/mmm)$, $D_{3h}(\bar{6}m2)$, $C_{6v}(6mm)$, $D_6(622)$, $C_{6h}(6/m)$, $C_{3h}(\bar{6})$ and $C_6(6)$ the only non-zero term of the fourth-rank absorption tensor is $\sigma^{Q}(4,0)$, so that

$$\begin{aligned}\sigma^{Q}(\hat{\varepsilon},\hat{k}) = \sigma^{Q}(0,0) &+ \sqrt{5/14}(3\sin^2\theta\sin^2\psi - 1)\sigma^{Q}(2,0) \\ &+ 1/\sqrt{14}(35\sin^2\theta\cos^2\theta\cos^2\psi \\ &+ 5\sin^2\theta\sin^2\psi - 4)\sigma^{Q}(4,0).\end{aligned} \tag{5.3}$$

(iii) For $D_{3d}(\bar{3}m)$ and $D_3(32)$, one has the further term $\sigma^{Q}(4,3) = -\sigma^{Q}(4,-3)$, so that $\sigma^{Qi}(4,3) = 0$ and

$$\begin{aligned}\sigma^{Q}(\hat{\varepsilon},\hat{k}) = \sigma^{Q}(0,0) &+ \sqrt{5/14}(3\sin^2\theta\sin^2\psi - 1)\sigma^{Q}(2,0) \\ &+ 1/\sqrt{14}(35\sin^2\theta\cos^2\theta\cos^2\psi + 5\sin^2\theta\sin^2\psi - 4)\sigma^{Q}(4,0) \\ &- \sqrt{10}\sin\theta[(2\cos^2\theta\cos^2\psi - 1)\cos\theta\cos(3\varphi) \\ &- (3\cos^2\theta - 1)\sin\psi\cos\psi\sin(3\varphi)]\sigma^{Qr}(4,3).\end{aligned} \tag{5.4}$$

(iv) For the symmetry group $C_{3v}(3m)\sigma^{Q}(4,3) = \sigma^{Q}(4,-3)$, so that $\sigma^{Qr}(4,3) = 0$ and

$$\begin{aligned}\sigma^{Q}(\hat{\varepsilon},\hat{k}) = \sigma^{Q}(0,0) &+ \sqrt{5/14}(3\sin^2\theta\sin^2\psi - 1)\sigma^{Q}(2,0) \\ &+ 1/\sqrt{14}(35\sin^2\theta\cos^2\theta\cos^2\psi + 5\sin^2\theta\sin^2\psi - 4)\sigma^{Q}(4,0) \\ &- \sqrt{10}\sin\theta[(2\cos^2\theta\cos^2\psi - 1)\cos\theta\sin(3\varphi) \\ &+ (3\cos^2\theta - 1)\sin\psi\cos\psi\cos(3\varphi)]\sigma^{Qi}(4,3).\end{aligned} \tag{5.5}$$

(v) For $S_6(\bar{3})$ and $C_3(3)$ there is no longer any additional relation between $\sigma^{Q}(4,3)$ and $\sigma^{Q}(4,-3)$ so that

$$\sigma^{Q}(\hat{\varepsilon}, \hat{k}) = \sigma^{Q}(0,0) + \sqrt{5/14}(3\sin^2\theta\sin^2\psi - 1)\sigma^{Q}(2,0)$$
$$+ 1/\sqrt{14}(35\sin^2\theta\cos^2\theta\cos^2\psi + 5\sin^2\theta\sin^2\psi - 4)\sigma^{Q}(4,0)$$
$$- \sqrt{10}\sin\theta[(2\cos^2\theta\cos^2\psi - 1)\cos\theta(\sigma^{Qr}(4,3)\cos(3\varphi)$$
$$+ \sigma^{Qi}(4,3)\sin(3\varphi)) - (3\cos^2\theta - 1)\sin\psi\cos\psi(\sigma^{Qr}(4,3)\sin(3\varphi)$$
$$- \sigma^{Qi}(4,3)\cos(3\varphi))]. \tag{5.6}$$

(vi) For the symmetry groups $D_{4h}(4/mmm)$, $D_{2d}(\bar{4}2m)$, $C_{4v}(4mm)$ and $D_4(422)$, one has $\sigma^{Q}(4,4) = \sigma^{Q}(4,-4)$ which yields $\sigma^{Qi}(4,4) = 0$ and

$$\sigma^{Q}(\hat{\varepsilon}, \hat{k}) = \sigma^{Q}(0,0) + \sqrt{5/14}(3\sin^2\theta\sin^2\psi - 1)\sigma^{Q}(2,0)$$
$$+ 1/\sqrt{14}[35\sin^2\theta\cos^2\theta\cos^2\psi + 5\sin^2\theta\sin^2\psi - 4]\sigma^{Q}(4,0)$$
$$+ \sqrt{5}\sin^2\theta[(\cos^2\theta\cos^2\psi - \sin^2\psi)\cos 4\varphi$$
$$- 2\cos\theta\sin\psi\cos\psi\sin 4\varphi]\sigma^{Qr}(4,4). \tag{5.7}$$

For example, $\cos^2\theta = (1/7)$ cancels the ψ-dependence of $\sigma^{Q}(4,0)$.

(vii) For the symmetry groups $C_{4h}(4/m)$, $S_4(\bar{4})$ and $C_4(4)$ there is no additional relation between $\sigma^{Q}(4,4)$ and $\sigma^{Q}(4,-4)$ so that

$$\sigma^{Q}(\hat{\varepsilon}, \hat{k}) = \sigma^{Q}(0,0) + \sqrt{5/14}(3\sin^2\theta\sin^2\psi - 1)\sigma^{Q}(2,0)$$
$$+ 1/\sqrt{14}[35\sin^2\theta\cos^2\theta\cos^2\psi + 5\sin^2\theta\sin^2\psi - 4]\sigma^{Q}(4,0)$$
$$+ \sqrt{5}\sin^2\theta[(\cos^2\theta\cos^2\psi - \sin^2\psi)(\cos(4\varphi)\sigma^{Qr}(4,4)$$
$$+ \sin(4\varphi)\sigma^{Qi}(4,4)) - 2\cos\theta\sin\psi\cos\psi(\sin(4\varphi)\sigma^{Qr}(4,4)$$
$$- \cos(4\varphi)\sigma^{Qi}(4,4))]. \tag{5.8}$$

For the other point groups, there are too many parameters to allow experimental determination. However, for completeness, the general formula is given in appendix 3. The additional relations given by the symmetries are listed below.

(viii) For the point groups $D_2(222)$, $C_{2v}(mm2)$ and $D_{2h}(mmm)$, one has $\sigma^{Qi}(2,2) = 0$, $\sigma^{Qi}(4,4) = \sigma^{Qi}(4,2) = 0$ and $\sigma^{Q}(2,m) = \sigma^{Q}(4,m) = 0$ for m odd.

(ix) For the point groups $C_2(2)$, $C_s(m)$ and $C_{2h}(2/m)$, one has only $\sigma^{Q}(2,m) = \sigma^{Q}(4,m) = 0$ for m odd.

(x) Finally, the most general angular dependence is found for the symmetry groups $C_1(1)$ (no symmetry) and $C_i(\bar{1})$ (inversion centre).

As expected, the number of independent parameters in each point group is that of a fully symmetric fourth-rank tensor [128].

5.2. *Experimental example*

The author knows of only two successful experimental works which have been carried out on the angular dependence of quadrupole absorption. The earliest one will be discussed later and the second one is presented now because it gives a good illustration of the way to plan angle-resolved experiments.

Dräger *et al* [129] have investigated the multipole character of the x-ray transitions at the iron K-edge of four single crystals. The results of the previous sections will be used to analyse their experiments.

For a cubic crystal (such as BCC Fe) the angular dependence only arises from the coefficient of $\sigma^Q(4,0)$ which varies from $-4/\sqrt{14}$ to $6/\sqrt{14}$. Since the electric quadrupole cross section $\sigma^Q(\hat{\varepsilon},\hat{k})$ is positive, the parameter $\sigma^Q(4,0)$ is restricted within $-(\sqrt{14}/6)\sigma^Q(0,0) \leqslant \sigma^Q(4,0) \leqslant (\sqrt{14}/4)\sigma^Q(0,0)$. This inequality shows that an angular dependence of quadrupole absorption of single crystals can be expected only if the spectrum of the corresponding powder exhibits appreciable quadrupole features ($\sigma^Q(0,0) \neq 0$). This is obvious since $\sigma^Q(0,0)$ is the angular average of positive $\sigma^Q(\hat{\varepsilon},\hat{k})$. The full range of angular values is obtained by choosing $\theta = \pi/2$ so that

$$\sigma^Q(\hat{\varepsilon},\hat{k}) = \sigma^Q(0,0) + 1/\sqrt{14}[10\sin^2\psi\sin^2 2\varphi - 4]\sigma^Q(4,0). \tag{5.9}$$

Therefore, the beam and polarisation directions ($\hat{k}\|[110]$, $\hat{\varepsilon}\|[1\bar{1}0]$ and $\hat{k}\|[110]$, $\hat{\varepsilon}\|[001]$) chosen by Dräger *et al* for the measurement of the quadrupole effect in cubic Fe and FeS_2 are optimal since they correspond to the maximum and minimum values of the angular coefficient of $\sigma^Q(4,0)$. However, they observe no angular dependence, so that the value of $\sigma^Q(4,0)$ is very small in BCC iron. This does not mean *a priori* that the quadrupole contribution $\sigma^Q(0,0)$ is negligible.

The same authors have also investigated the angular dependence of haematite (α-Fe_2O_3) and siderite ($FeCO_3$), whose point group is D_{3d}. They have conducted four experiments (figure 1) corresponding to the following wavevector and polarisation directions (expressed in hexagonal indices):

(1) $\hat{k}\|[12.0]$, $\hat{\varepsilon}\|[10.0]$ so that $\theta = \pi/2$, $\psi = \pi/2$, $\varphi = 0$ and

$$\sigma_1 = \sigma^D(0,0) + 1/\sqrt{2}\sigma^D(2,0) + \sigma^Q(0,0) + 2\sqrt{5/14}\sigma^Q(2,0) + 1/\sqrt{14}\sigma^Q(4,0). \tag{5.10}$$

(2) $\hat{k}\|[12.0]$, $\hat{\varepsilon}\|[00.1]$ so that $\theta = 0$, $\psi = 0$, $\varphi = \pi/2$ and

$$\sigma_2 = \sigma^D(0,0) - \sqrt{2}\sigma^D(2,0) + \sigma^Q(0,0) - \sqrt{5/14}\sigma^Q(2,0) - 4/\sqrt{14}\sigma^Q(4,0). \tag{5.11}$$

(3) $\hat{k}\|[00.1]$, $\hat{\varepsilon}\|[10.0]$ so that $\theta = \pi/2$, $\psi = \pi$, $\varphi = 0$ and

$$\sigma_3 = \sigma^D(0,0) + 1/\sqrt{2}\sigma^D(2,0) + \sigma^Q(0,0) - \sqrt{5/14}\sigma^Q(2,0) - 4/\sqrt{14}\sigma^Q(4,0). \tag{5.12}$$

(4) $\hat{k}\|[00.1]$, $\hat{\varepsilon}\|[12.0]$ so that $\theta = \pi/2$, $\psi = \pi$, $\varphi = \pi/2$ and

$$\sigma_4 = \sigma^D(0,0) + 1/\sqrt{2}\sigma^D(2,0) + \sigma^Q(0,0) - \sqrt{5/14}\sigma^Q(2,0) - 4/\sqrt{14}\sigma^Q(4,0). \tag{5.13}$$

Therefore, $\sigma_3 = \sigma_4$ and

$$\sigma_1 - \sigma_3 = 3\sqrt{5/14}\sigma^Q(2,0) + 5/\sqrt{14\sigma^Q}(4,0)$$

is purely quadrupole,

$$\sigma_2 - \sigma_4 = -3/\sqrt{2}\sigma^D(2,0)$$

is purely dipole.

In the Fe K-edge spectra of haematite plotted in figure 1, the value of $\sigma_2 - \sigma_4$ shows that there is a strong dipole character at the pre-edge feature which is usually attributed to $1s \rightarrow 3d$ transitions. In other words, the final-state wavefunction has a relatively large p component that indicates the presence of p and d state in that energy range. The existence of a non-zero quadrupole component $\sigma_1 - \sigma_3$ proves that there are indeed d states within the energy range of the pre-peaks of the haematite spectra.

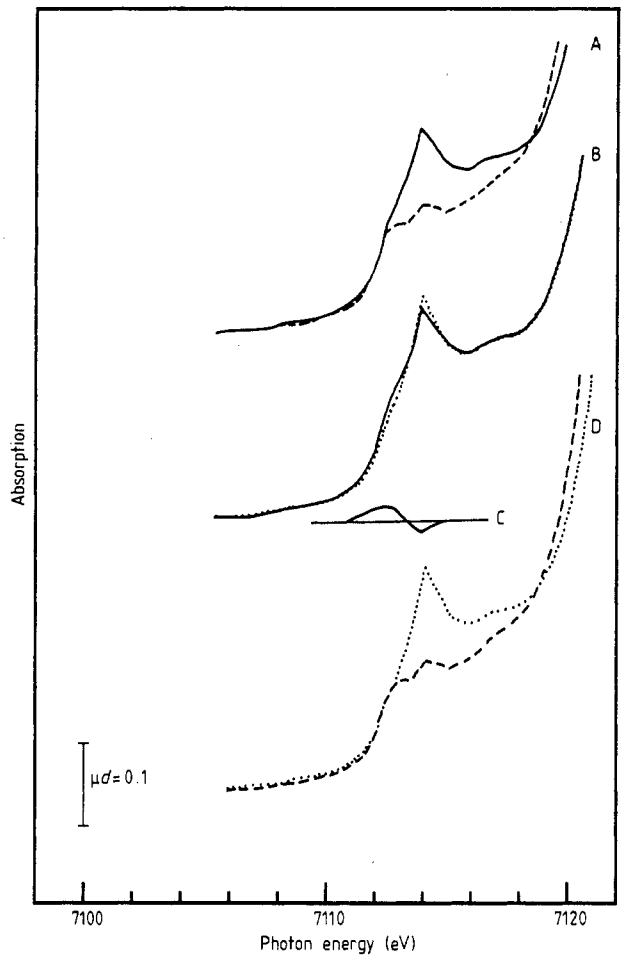

Figure 1. The angular dependence of the pre-edge Fe K absorption of α-Fe_2O_3: A for $\hat{k} \| [12.0]$, $\hat{\varepsilon} \| [10.0]$ (——) and $\hat{\varepsilon} \| [00.1]$ (– – –); B with the same $\hat{\varepsilon} \| [10.0]$ position, but for $\hat{k} \| [12.0]$ (——) and [00.1] (· · · · ·); C the difference between the latter curves; D for interchanged $\hat{k}$ and $\hat{\varepsilon}$, i.e. $\hat{k} \| [12.0]$, $\hat{\varepsilon} \| [00.1]$ (– – –) and $\hat{k} \| [00.1]$, $\hat{\varepsilon} \| [12.0]$ (· · · · ·) (taken from [129]).

Additional measurements would be necessary in order to extract all the tensor components of the angle-dependent absorption spectra. To measure all the parameters, the following procedure is possible. (i) Measure a powder to obtain $\sigma^D(0,0) + \sigma^Q(0,0)$. Note that it is never possible to separate $\sigma^D(0,0)$ from $\sigma^Q(0,0)$ without further hypotheses. (ii) Turn the sample around the crystal c axis to measure $\sigma^{Qr}(4,3)$. Do not align the x-ray beam with the c axis because no angular dependence is found in that case, and this is generally true for n-fold symmetric samples with n greater than two. (iii) Take $\cos^2\theta = 1/3$ (magic angle) and $\sin^2\psi = 1/2$ to measure $\sigma^Q(4,0)$. (iv) Take $\cos^2\theta = 1/3$ and $\sin^2\psi \neq 1/2$ to measure $\sigma^Q(2,0)$. (iv) Take $\cos^2\theta \neq 1/3$ to measure $\sigma^D(2,0)$.

In any case, it is better to measure a large number of angles, so that the tensor components can be deduced by fitting the experimental results to the theoretical angular

dependence. The determination of $\sigma^{D,Q}(l,m)$ by a fitting procedure is particularly easy with formulae (4.4)–(4.7) and (5.2)–(5.8) since the observed spectrum is written as a linear combination of tensor components $\sigma^{D,Q}(l,m)$.

6. Physical interpretation in terms of molecular orbitals

In the previous section it was shown that, within a one-electron interpretation, the p and d components of the final-state wavefunction can be measured from angle-dependent spectra. This is a particular feature of K-edge core-level absorption: since the initial 1s state is spherically symmetric, the selection rules ensure that the dipole transition will pick up the p component of the final state whereas the quadrupole transition will select the d component of the photoelectron wavefunction. The smallness of the d component observed is due to the amplitude of quadrupole transitions, which is much smaller than that of dipole transitions. The additional advantage of angle-dependent spectra is the possibility of obtaining selective information on the p_x, p_y and p_z components of the final state (for dipole transitions from a K-edge) by aligning the polarisation vector along the x, y and z axes, respectively. This type of analysis was used to study the shake-down phenomena in copper complexes [130–132] and it enabled two groups to determine the symmetry of the oxygen holes in high-T_c superconductors [110, 133]. In this section it is shown how the tensor components can be connected to the molecular orbital description of the final state, using the remarkable measurements conducted by Hahn *et al* [134] at the copper K-edge of $CuCl_4^{2-}$. The symmetry of the molecule is approximately D_{4h}. The x-ray beam and the polarisation were in the (a,b) plane ($\theta = \psi = \pi/2$) so that the angular dependence is

$$\sigma(\hat{\varepsilon},\hat{k}) = \sigma^{D}(0,0) + 1/\sqrt{2}\sigma^{D}(2,0) + \sigma^{Q}(0,0) + 2\sqrt{5/14}\sigma^{Q}(2,0) + 1/\sqrt{14}\sigma^{Q}(4,0) - \sqrt{5}\cos 4\varphi\,\sigma^{Qr}(4,4). \tag{6.1}$$

This angular dependence is perfectly consistent with the experimental data (figure 2).

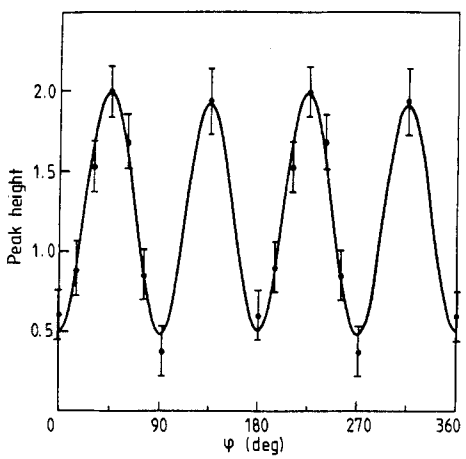

Figure 2. Angular dependence of 1s → 3d transition in square-planar $CuCl_4^{2-}$. Cross section (arbitrary units) as a function of rotation angle φ about the crystal c axis (data were actually collected for φ values of 0–180°) (taken from [82]).

The authors make the further assumption that a molecular orbital describes the final state accurately. This leads to the following conclusions. If we define

$$\sigma^{D}(1,\mu,1,\mu') = -\pi\alpha\hbar\omega(4\pi/3)^2\sqrt{3}\sum_{if}\langle i|rY_1^{\mu}(\hat{r})|f\rangle\langle f|rY_1^{\mu'}(\hat{r})|i\rangle\delta(E_f - E_i - \hbar\omega) \tag{6.2}$$

and

$$\sigma^{Q}(2,\nu,2,\nu') = 3\pi\alpha\hbar\omega k^2/(20\sqrt{5})\sum_{if}\langle i|r^2Y_2^{\nu}(\hat{r})|f\rangle\langle f|r^2Y_2^{\nu'}(\hat{r})|i\rangle\delta(E_f - E_i - \hbar\omega) \tag{6.3}$$

we obtain, according to appendix 1,

$$\sigma^{D}(l,m) = \sum_{\mu\mu'}(1\mu1\mu'|lm)\sigma^{D}(1,\mu,1,\mu') \quad \text{or} \quad \sigma^{D}(1,\mu,1,\mu') = \sum_{lm}(1\mu1\mu'|lm)\sigma^{D}(l,m) \tag{6.4}$$

and

$$\sigma^{Q}(l,m) = \sum_{\nu\nu'}(2\nu2\nu'|lm)\sigma^{Q}(2,\nu,2,\nu') \quad \text{or} \quad \sigma^{Q}(2,\nu,2,\nu') = \sum_{lm}(2\nu2\nu'|lm)\sigma^{Q}(l,m). \tag{6.5}$$

The coefficients $\sigma^{Q}(2,\nu,2,\nu')$ can also be used as parameters of the angular dependence of x-ray absorption spectra. Somehow, $\sigma^{Q}(2,\nu,2,\nu')$ gives a more immediate description of the final state reached by the photoelectron. The tensor components $\sigma^{Q}(l,m)$ are preferred because they make the crystalline symmetries much easier to account for. In any case, relations (6.4) and (6.5) between the two descriptions are made very simple by the square-root factors included in the angular dependences (A4) and (A8).

Let us follow the reasoning of Hahn *et al* with the present notation. They assume that the only available final state at the pre-edge energy is a pure $d_{x^2-y^2}$ orbital, so that the angular part of the final state is given by

$$|f\rangle = |d_{x^2-y^2}\rangle \propto (Y_2^2(\hat{r}) + Y_2^{-2}(\hat{r})). \tag{6.6}$$

Then, since they measured a K-edge, $|i\rangle$ is a 1s orbital and $\langle i|rY_1^{\mu}(\hat{r})|f\rangle = 0$, so that all $\sigma^{D}(1,\mu,1,\mu')$ are zero and the dipolar absorption vanishes. For quadrupolar absorption, (6.3) yields $\sigma^{Q}(2,2,2,2) = \sigma^{Q}(2,2,2,-2) = \sigma^{Q}(2,-2,2,2) = \sigma^{Q}(2,-2,2,-2) \equiv \zeta$. Hence, according to (6.5) we find the tensor components: $\sigma^{Qr}(4,4) = \sigma^{Qr}(4,-4) = \zeta$, $\sigma^{Q}(4,0) = 2\zeta/\sqrt{70}$, $\sigma^{Q}(2,0) = 4\zeta/\sqrt{14}$, $\sigma^{Q}(0,0) = 2\zeta/\sqrt{5}$, and the angular dependence becomes

$$\sigma(\hat{\varepsilon},\hat{k}) = \sqrt{5}(1 - \cos 4\varphi)\zeta \tag{6.7}$$

i.e. that obtained by Hahn *et al*.

Now, there is a problem because the experimental absorption cross section is not zero when $\cos 4\varphi = 1$. The authors ascribe this discrepancy to the slight misalignment of the two molecules per cell and to vibronically allowed dipole transitions. In fact, the molecular-orbital picture is an approximation compared with formula (6.1) and a departure from a pure one-electron $d_{x^2-y^2}$ final state could also explain this discrepancy. Anyway, the dipole/quadrupole nature of the remaining peak can be tested with further

angular-dependent absorption spectra, and its vibronic origin could be probed by temperature-dependent measurements, as noted in reference [134].

The assumption that there is only one molecular orbital available restricts the tensor components of the absorption considerably. Since there is only one term in the sum over $|f\rangle$, all the $\sigma^D(1,\mu,1,\mu')$ are proportional to a product of the term $\langle i|rY_1^{\mu}(\hat{r})|f\rangle$ by the term $\langle f|rY_1^{\mu'}(\hat{r})|i\rangle$ (whereas in the general case $\Sigma_f|\langle i|T|f\rangle|^2 \neq |\Sigma_f\langle i|T|f\rangle|^2$, where T is a transition operator). Therefore, since $\langle i|rY_1^{-\mu'}(\hat{r})|f\rangle = (-1)^{\mu'}\langle f|rY_1^{\mu'}(\hat{r})|i\rangle^*$ there are now three independent parameters (the real and imaginary parts of $\langle i|rY_1^{\mu}(\hat{r})|f\rangle$) instead of six for the trichroism class (iiic). The same is true of quadrupolar absorption. If there is only one molecular orbital available, there are five parameters instead of 15 for the most general angular dependence. The isotropic component observed by Hahn *et al* could be due to the presence of several final states at the same energy. The fact that the incident x-rays are never perfectly polarised is also relevant here.

With the foregoing example, a direct connection is established between the spherical tensor parametrisation of the angular dependence and the atomic- or molecular-orbital approach which was used by many workers to interpret angle-resolved x-ray absorption spectra [21, 66, 110, 111, 117, 130–149, 222]. The Clebsch–Gordan coefficients necessary for linking tensor components to molecular-orbital results are listed in appendix 4. Note that when ligand effects are appreciable, the ligand wavefunctions must be expanded around the photoabsorbing centre. For dipole (quadrupole) K-edge absorption, the $l = 1$ ($l = 2$) components of the expansion are picked up by the selection rule. Standard methods exist to carry out such single-centre expansions [150, 151]. The above example shows also that, with angle-resolved XAS, it is possible to check whether there is only one accessible molecular orbital, provided the other causes of discrepancy, such as misalignment or vibronic transitions, have been discarded.

Within the one-electron picture of the x-ray absorption process, one can also understand the difference between a quadrupole absorption at an L_I-edge and a dipole absorption at an L_{II}- or L_{III}-edge. In the former case, one studies the pure d component of the final-state wavefunction, whereas in the latter case only mixed s and d information is available. The K-edge spectra measure the value of the final-state wavefunctions near the nucleus, while for L-edges, the initial state is not so localised. Moreover, quadrupole absorption can yield more information since a cubic crystal may exhibit quadrupole angular dependence, whereas the dipole absorption is isotropic. Since the angular dependences of quadrupole and dipole transitions are always different, it is possible to prove the quadrupolar nature of some pre-edge features (e.g. in the K-edge of transition-metal compounds) which are often ascribed to quadrupole transitions without definite evidence.

Natoli [152] established that, when the interatomic distances R in a cluster of atoms are modified, the energy position of the XAS peaks shift by ΔE according to the rule $(E + \Delta E)(R + \Delta R)^2 = ER^2$. Since Natoli's derivation applies to the whole scattering path operator, all the tensor components follow the $1/R^2$ scaling (within the domain of validity of this rule). This was verified experimentally for some transition-metal complexes [139–141, 153].

7. Experimental aspects

In this section some of the problems encountered in the experimental investigation of the angular dependence of x-ray absorption spectra are discussed.

7.1. Polarisation of the incident x-rays

As already noted by Fresnel in 1821, the existence of unpolarised waves is a serious problem for classical optics (in modern terms every solution of Maxwell's equations which propagates spatially as a plane wave is necessarily completely polarised). Thus, the concept of an unpolarised wave involves quantal considerations (reference [36] p 453). In practice, the x-rays incident on the sample are never completely polarised. The concept of wave polarisation is thoroughly discussed in §10.8 of reference [37]. In particular, it can be shown that any quasi-monochromatic light wave may be regarded as the sum of a completely unpolarised and a completely polarised wave. Let the degree of polarisation P be the ratio of the intensity of the completely polarised wave over the total intensity of the wave. At the centre of the synchrotron radiation beam, the completely polarised wave can be considered to be linearly polarised parallel to the electron/positron orbit plane. Then the degree of polarisation can be measured with standard methods [154] and is often around 95%. In an experimental procedure, it may be useful to move the slits vertically and record the spectra in such a way that the maximum intensity of the anisotropic components of the spectra is obtained at the centre of the beam.

From equation (3.16), the absorption cross section can be written

$$\sigma(\hat{\varepsilon}) = \sum_{ij} \varepsilon_i \varepsilon_j^* \sigma^{ij} = \mathrm{Tr}\{\boldsymbol{\rho}\boldsymbol{\sigma}\} \tag{7.1}$$

where $\boldsymbol{\rho} = \{\varepsilon_i \varepsilon_j^*\}$ is the density matrix [36] or coherency matrix [37] describing the polarisation state of the incident x-ray beam. The matrix $\boldsymbol{\sigma}$ describes the absorption, and can be written as the sum of dipole and quadrupole contributions, $\boldsymbol{\sigma} = \boldsymbol{\sigma}^{\mathrm{D}} + \boldsymbol{\sigma}^{\mathrm{Q}}$, that are given in appendix 3.

Equation (7.1) is valid when the incident x-ray can be described by the sum of a completely linearly polarised and a completely unpolarised beam. This is the general case for synchrotron radiation in the plane of the electron/positron orbit. If one defines the x-ray and polarisation directions in the crystal reference frame by

$$\hat{k} = \begin{pmatrix} \sin\theta\cos\varphi \\ \sin\theta\sin\varphi \\ \cos\theta \end{pmatrix} \qquad \hat{\varepsilon} = \begin{pmatrix} \cos\theta\cos\varphi\cos\psi - \sin\varphi\sin\psi \\ \cos\theta\sin\varphi\cos\psi + \cos\varphi\sin\psi \\ -\sin\theta\cos\psi \end{pmatrix} \tag{7.2}$$

where $\psi = 0$ and $\psi = \pi/2$ correspond to a linear polarisation along x and y respective to a reference frame where the x-ray wavevector is along Oz. Then, if P is the degree of polarisation of the beam, the polarisation density matrix of the incident x-rays is

$$\boldsymbol{\rho} = (1/2)\begin{bmatrix} 1 + P\cos 2\psi & P\sin 2\psi \\ P\sin 2\psi & 1 - P\cos 2\psi \end{bmatrix}. \tag{7.3}$$

An interesting conclusion of this treatment is that angle-resolved XAS can be done with completely unpolarised x-rays. Equation (7.1) applied to the density matrix of unpolarised x-rays gives, for the dipole absorption contribution,

$$\sigma^{\mathrm{D}}(\hat{k}) = \sigma^{\mathrm{D}}(0,0) + \sqrt{2\pi/5} \sum_{m=-2}^{2} Y_2^{m*}(\hat{k})\sigma^{\mathrm{D}}(2,m). \tag{7.4}$$

Therefore, all the parameters of the angular dependence of XAS are measurable with unpolarised x-rays but the magnitude of the effect is divided by two. This was predicted by Izraileva [52] and observed on Ga [30, 49, 53, 155, 156] and $Cu_{0.5}NbS_2$ [93]. Since the polarisation direction must be orthogonal to the x-ray wavevector, averaging over polarisation directions (to obtain unpolarised rays) is not the same as averaging over all directions (as in a powder). This angular effect should not be overlooked when measuring single-crystals or oriented powders with conventional x-ray sources.

The effect of circularly polarised light must also be mentioned. Since the dipole absorption of left- and right-circularly polarised x-rays is identical [157], equation (7.1) still applies to σ^D for circularly polarised x-rays and thus to any polarisation. The angular dependence of the dipole absorption by pure circularly polarised x-rays is the same as that for unpolarised beams. The case of quadrupole absorption is a little more involved. If the sample under study has specific symmetry operations (e.g. a centre of inversion), then the equation $\boldsymbol{\sigma} = \boldsymbol{\sigma}^D + \boldsymbol{\sigma}^Q$ remains valid for general polarisation. However, for certain single crystals, there can be an interference between the dipole and the quadrupole matrix elements in the square modulus of expression (3.15). Then, the angular dependence of the absorption by circularly polarised light is more complex and would require a separate treatment. This interference is a source of natural circular dichroism [157]. It should be stressed that all this discussion applies only when no magnetic field (internal or external) is present.

7.2. *Experimental problems*

7.2.1. Textured samples. When measuring oriented polycrystals or oriented powders, some of the tensor components of the x-ray absorption spectra can still be observed. It was shown by Pettifer *et al* [112] that the Cu K-edge spectrum of $La_{1.85}Ba_{0.15}CuO_4$ powders (which were not oriented deliberately) exhibits an angular variation, the intensity of which increases with the average grain size. Generally, for textured samples, the observable tensor components are calculated by averaging the single-crystal $\sigma(l, m)$ over the crystallite orientation distribution, which can be determined by standard methods [158]. For example, if the orientation distribution is uniaxial (which is generally the case for powders), the anisotropic tensor components $\sigma^D(2, 0)$, $\sigma^Q(2, 0)$ and $\sigma^Q(4, 0)$ can be deduced from experimental spectra.

7.2.2. Diffraction peaks. The study of single crystals is often seriously complicated by the presence of diffraction peaks. In this case, information about the angular dependence of the x-ray absorption spectra can still be obtained by rotating the sample [159]. For instance, by rotating the sample around its c axis one can observe the $m = 0$ components of the absorption tensors. The $m \neq 0$ components can also be measured by properly choosing the rotation axes.

7.2.3. Background effects and normalisation. In the fluorescence detection of EXAFS, the background signal is due to scattered radiation. The intensity of this radiation is greatly affected by the polarisation of the incident beam and by the detector position. This effect was discussed and calculated by Sandstrom and Fine [160].

In transmission experiments one must turn the samples around various axes. Usually, this changes the sample thickness crossed by the x-ray beam and it is necessary to suppress harmonics with a mirror and to keep the total absorption μd small to avoid the so called 'thickness effect' [19]. Another problem met in transmission experiments is the

presence of pinholes or cracks due to the thinness of the sample. Homogeneity can be checked by translating the sample in the x-ray beam and by verifying that the edge jump is proportional to the thickness crossed by the beam. The background can also be affected by diffraction anisotropy [161] but this effect is relatively small, confined to specific energies and can be estimated with dynamic theory [161].

Normalisation is an important step of the analysis. It is made easier when sparse data are recorded over a wide range around the edge (e.g. from 500 eV before to 2000 eV after the edge). As noted above, in energy regions where the quadrupole contribution is expected to be small, all the spectra should cross at points where $\sigma^{D}(2, 0) = 0$. This provides a check that normalisation is correct.

7.2.4. Crystal orientation and energy calibration. For fitting theoretical angular dependence (equations (4.3)–(4.7) and (5.2)–(5.8)) to experimental spectra, the orientation of the x-ray wavevector and polarisation in the crystal reference frame must be known accurately. The accuracy depends on the effect investigated. When studying dipole angular variations, which are typically of the order of 10% of the edge jump, the orientations must be known to an accuracy around 2°. Quadrupole angular effects are much smaller and require a thorough determination of x-ray beam and crystal axes orientations, with an accuracy better than one degree. The polarisation direction can be considered to be constant through the sample since the rotation of the polarisation was shown to be very small in the x-ray range [162]. An energy shift can also spoil measurements, so an energy calibration must be made frequently with a reference sample.

7.2.5. Temperature. Vibronic transitions are not taken into account by the present formalism. They have not been evidenced unequivocally in XAS but their eventual occurrence can be minimised by working at low temperature.

8. Conclusion

In this paper, a detailed account of the angular dependence of x-ray absorption spectra was presented, including the electric dipole and electric quadrupole effects. Since each of these terms represents a transition to different angular momenta, it is important to be able to distinguish them. By carefully choosing the x-ray beam, polarisation and sample orientations, it is possible to extract quadrupolar parameters, which are most important, for instance in the study of the density of d states in transition metals. Detailed formulae were provided to analyse the experimental spectra in terms of two theoretical descriptions of the absorption process: the molecular-orbital and the multiple-scattering approaches corresponding to bound and continuum final states, respectively (an alternative interpretation in terms of crystal-field theory was proposed by Starke *et al* [163]).

The angular dependence of x-ray absorption spectra can also be used to orientate a single crystal or to measure the linear components of the polarisation of an x-ray beam in various directions with a highly anisotropic reference crystal, such as a transition-metal complex (e.g. [131, 136, 138–140]). It allows the interpolation of spectra which cannot be obtained experimentally (for instance with the x-ray beam parallel to the surface).

The angular dependence obtained is very general since it includes spin–orbit and many-body effects and does not depend on whether the final state is described as a bound

or continuum state. However, it does not take into account the lattice distortions which break the crystal point-group symmetries. Conversely, the presence of an angular dependence which is forbidden by the point group may indicate that the crystal is distorted. It should be stressed again that the present derivation does not apply to magnetic samples. Therefore, magnetic x-ray dichroism observed with linear or circular polarisation [164, 165] does not, in general, satisfy the formulae given here.

Although almost no mention was made of the surface x-ray absorption spectroscopy, the angular dependence described above is also valid for molecules and can be useful to determine the orientation of molecules on substrates [115, 149].

Acknowledgments

This article has been much improved by the comments received from Professors G Krill and M Gerl. The questions of circular dichroism and magnetic dipole transitions in the x-ray range have been clarified with the help of Drs J Goulon and M Loos. Professor R F Pettifer has pointed out to me the early experiments carried out to study the angular dependence of cubic single crystals. The molecular-orbital interpretation of the quadrupole transition has been thoroughly discussed with Dr B Poumellec. Section 3.2 and tables 1 to 4 owe much to the reprints supplied by Drs J P Briand, G Dräger, J E Penner-Hahn, R Frahm, T A Tyson, G Loupias, E Dartyge, A-M Flank, P Sainctavit, A Fontaine, H Tolentino, G Tourillon, N Kosugi, A Manceau, A Petcov and D Norman. The English was polished by Dr P E J Hoggan. Let them all be warmly thanked.

Appendix 1. X-ray absorption cross section and symmetries

The present appendix is devoted to the study of the tensor properties of the dipole and quadrupole transitions. When these properties are established, the power of group theory will simplify the expression of the angular dependence of x-ray absorption spectra considerably. Since the initial and final states are not specified, the final results are completely general, including many-body effects. Firstly, the dipole transition is dealt with, then the more difficult quadrupole transition is treated. Some of these problems were solved very elegantly by Stedman using the diagram notation for the quantum theory of angular momentum [166]. However, since this diagrammatic representation is highly abstract, standard angular momentum theory is preferred here.

A1.1. Dipole transitions

The dipole absorption cross section can be written

$$\sigma^{D}(\hat{\varepsilon}) = 4\pi^2\alpha\hbar\omega \sum_{if} |\langle f|\,\hat{\varepsilon}\cdot\boldsymbol{r}\,|i\rangle|^2\delta(E_f - E_i - \hbar\omega) = \sum_{ij} \varepsilon_i\varepsilon_j\sigma^{ij}. \qquad (A1)$$

It is physically obvious that rotating or translating the sample *and* the x-ray polarisation does not change the absorption cross section. Therefore, σ^{ij} is a symmetric Cartesian tensor of rank 2 [167]. Repeating the calculation of the polarised absorption cross section

carried out in reference [98], we find, with the notation of appendix 2,

$$\sigma^{\mathrm{D}}(\hat{\varepsilon}) = 4\pi^2\alpha\hbar\omega(4\pi/3)^2 \sum_{l=0,2} \sum_{m=-l}^{l} Y_l^{m*}(\hat{\varepsilon})\langle l\|1\|1\rangle \sum_{\mu\mu'} (1\mu 1\mu'|lm)$$
$$\times \sum_{\mathrm{if}} \langle \mathrm{i}|rY_1^{\mu}(\hat{r})|\mathrm{f}\rangle\langle \mathrm{f}|rY_1^{\mu'}(\hat{r})|\mathrm{i}\rangle\delta(E_{\mathrm{f}} - E_{\mathrm{i}} - \hbar\omega). \tag{A2}$$

Since the initial- and final-state wavefunctions can be chosen real, the sum over final states is symmetric in μ, μ':

$$\sum_{\mathrm{if}} \langle \mathrm{i}|rY_1^{\mu}(\hat{r})|\mathrm{f}\rangle\langle \mathrm{f}|rY_1^{\mu'}(\hat{r})|\mathrm{i}\rangle = \sum_{\mathrm{if}} \langle \mathrm{i}|rY_1^{\mu'}(\hat{r})|\mathrm{f}\rangle\langle \mathrm{f}|rY_1^{\mu}(\hat{r})|\mathrm{i}\rangle. \tag{A3}$$

Now we introduce the quantity $\sigma^{\mathrm{D}}(l, m)$ which is the mth component of a spherical tensor of rank l (i.e. it transforms as the spherical harmonic $Y_l^m(\hat{r})$). $\sigma^{\mathrm{D}}(l, m)$ will be the parameters of the spherical tensor expansion of the dipole contribution to the absorption cross section. Normalising $\sigma^{\mathrm{D}}(l, m)$ so that the coefficient of the isotropic term ($\sigma^{\mathrm{D}}(0, 0)$) is unity, we obtain

$$\sigma^{\mathrm{D}}(\hat{\varepsilon}) = \sigma^{\mathrm{D}}(0, 0) - \sqrt{8\pi/5} \sum_{m=-2}^{2} Y_2^{m*}(\hat{\varepsilon})\sigma^{\mathrm{D}}(2, m). \tag{A4}$$

where

$$\sigma^{\mathrm{D}}(l, m) = -\pi\alpha\hbar\omega(4\pi/3)^2\sqrt{3} \sum_{\mu\mu'} (1\mu 1\mu'|lm)$$
$$\times \sum_{\mathrm{if}} \langle \mathrm{i}|rY_1^{\mu}(\hat{r})|\mathrm{f}\rangle\langle \mathrm{f}|rY_1^{\mu'}(\hat{r})|\mathrm{i}\rangle\delta(E_{\mathrm{f}} - E_{\mathrm{i}} - \hbar\omega). \tag{A5}$$

This way of writing the absorption cross section is very convenient because it shows the angular dependence clearly. The first term $\sigma^{\mathrm{D}}(0, 0)$ is a $(0, 0)$ spherical tensor (invariant under rotation). In other words, it is the spectrum obtained on a powder. The second term $\sigma^{\mathrm{D}}(l, m)$ expresses the angular dependence. The factor $-\sqrt{8\pi/5}$ is used to give a simple relation between the tensor components $\sigma^{\mathrm{D}}(l, m)$ and the molecular-orbital description of the absorption cross section (see § 6).

A1.2. Quadrupole transitions

The quadrupole absorption cross section is

$$\sigma^{\mathrm{Q}}(\hat{\varepsilon}, \boldsymbol{k}) = \pi^2\alpha\hbar\omega \sum_{\mathrm{if}} |\langle \mathrm{f}|\hat{\varepsilon}\cdot\boldsymbol{r}\boldsymbol{k}\cdot\boldsymbol{r}|\mathrm{i}\rangle|^2\delta(E_{\mathrm{f}} - E_{\mathrm{i}} - \hbar\omega) = \sum_{ijkl} \varepsilon_i\varepsilon_j k_k k_l \sigma^{ijkl}. \tag{A6}$$

σ^{ijkl} is now a symmetric fourth-rank Cartesian tensor. To transform Cartesian tensors into spherical tensors, there is a standard procedure that was used for instance by Gaisenok [168] to calculate the angular dependence of multiphoton processes. As explained in appendix 2 within the multiple-scattering framework, the fourth-rank Cartesian absorption tensor can be expanded over spherical tensors $\sigma^{\mathrm{Q}}(l, m)$ with azimuthal quantum numbers l varying from 0 to 4. Because of the symmetry of $\sigma^{\mathrm{Q}}(\hat{\varepsilon}, \boldsymbol{k})$, the odd components ($l = 1$ and 3) are zero. The final result is (the notation is defined in appendix 2):

$$\sigma^{\mathrm{Q}}(\hat{\varepsilon}, \boldsymbol{k}) = (4\pi/3)^2 2\sqrt{5} \sum_{abl} B(a, b, l) \sum_{\alpha\beta m} (a\alpha b\beta|lm) Y_a^{\alpha*}(\hat{\varepsilon}) Y_b^{\beta*}(\hat{k}) \sigma^{\mathrm{Q}}(l, m) \tag{A7}$$

or, in expanded form,

$$\sigma^{Q}(\hat{\varepsilon}, \boldsymbol{k}) = \sigma^{Q}(0,0) + \sum_{m}\Big((-2/9)\sqrt{14\pi}[Y_2^{m*}(\hat{\varepsilon}) + Y_2^{m*}(\hat{k})] - 8\pi/(9\sqrt{5}) \times \sum_{\alpha\beta}(2\alpha 2\beta|2m)Y_2^{\alpha*}(\hat{\varepsilon})Y_2^{\beta*}(\hat{k})\Big)\sigma^{Q}(2,m) + \sum_{m}\Big(16\pi/(3\sqrt{5}) \times \sum_{\alpha\beta}(2\alpha 2\beta|4m)Y_2^{\alpha*}(\hat{\varepsilon})Y_2^{\beta*}(\hat{k})\Big)\sigma^{Q}(4,m) \tag{A8}$$

with

$$\sigma^{Q}(l,m) = 4\pi^3\alpha\hbar\omega k^2/(15\sqrt{5})\sum_{\nu\nu'}(2\nu 2\nu'|c\gamma) \times \sum_{if}\langle i|r^2Y_2^{\nu}(\hat{r})|f\rangle\langle f|r^2Y_2^{\nu'}(\hat{r})|i\rangle\delta(E_f - E_i - \hbar\omega). \tag{A9}$$

A1.3. Symmetry transformations

The tensor expansion allows a simple expression of the symmetries of the crystal to be written. The spherical tensor component $\sigma(l, m)$ transforms under rotation as the spherical harmonic $Y_l^m(\hat{r})$. It can be proved that $\sigma^{D}(\hat{\varepsilon})$ and $\sigma^{Q}(\hat{\varepsilon}, \boldsymbol{k})$ are invariant under the symmetry operations of the full point group of the crystal space group [169]. Therefore, the symmetries of the crystal can easily be taken into account. To do this, one first notes that the absorption by an atomic species in a molecule is the average of the absorption by all the atoms of this species and the average cross section is given by the average of the quantities $\sigma(l, m)$ over all equivalent sites of the molecule. Because of the transformation laws of spherical tensors (equation (3.215) of reference [36]), the averaged tensor components are:

$$\langle\sigma(l,m)\rangle = (1/N)\sum_{R}\sum_{m'}D^{l}_{m'm}(R^{-1})\sigma(l,m') \tag{A10}$$

where the sum over R is the sum over all the N symmetry operations of the crystal point group. Inversions do not change $\sigma(l, m)$ because there is an even number of r factors in (A1) and (A6). R has been used to designate the symmetry operations because the translations and inversions play no role and the proper rotation of each symmetry operation is taken for R. Moreover, R^{-1} has been written instead of R to emphasise that coordinates and tensors must be operated on with inverse rotations (p 93 of reference [36]). These transformation laws of the absorption cross section of crystals were already stated by Alexander *et al* [11]. Since the symmetry group of the electric dipole and quadrupole cross sections is the point group of the sample space group, it will be sufficient to list the angular dependence of the absorption cross section for all the point groups.

Equation (A10) is very convenient to calculate the influence of symmetries on the angular dependence of the absorption cross section with a computer. However, to investigate the same problem by hand, it is better to use the following idea. If one rotates the polarisation and x-ray wavevector directions according to a symmetry operation of the crystal, then one should obtain the same angular dependence as before the rotation and it is necessary to carry out this procedure for the generators of the group only. For instance, a rotation of angle γ around the z axis corresponds to the transformation $\phi \rightarrow \phi + \gamma$ in the general formulae (A38) and (4.7). In the case of the symmetry group C_4, a generator of the symmetries is given by $\gamma = \pi/2$, and one obtains an identical

formula after the transformation $\phi \rightarrow \phi + \pi/2$ in (A38) if and only if $\sigma^{Q}(l, m) = 0$ for $m \neq 0, 4$ or -4. This is the result (5.8).

Here, it is assumed that the wavefunctions $|i\rangle$ and $|f\rangle$ share the symmetry of the crystal, i.e. the spin and magnetic effects have been neglected. The rotational part of each crystal symmetry operation is used, even when it involves a translation. This may be surprising since the translational symmetry of the crystal is broken by the absorption process (the photoabsorber can be considered localised). However, all the equivalent atoms have the same probability of being photoexcited, and the absorption measured is summed over all the atoms of the same species in the crystal. This restores the full crystal symmetry. In the case of molecular crystals, the symmetry of the local environment of an atom may be higher than that of the crystal (e.g. the Fe environment in sodium nitroprusside [75]); in that case one must consider also the point group of that higher symmetry. This may enable one to discriminate between two atoms of the same species at different sites [138]. If one atom has a very high symmetry and the other has not, some of the angular dependence of the spectra will come only from the atom with low-symmetry surroundings.

Moreover, since $\sigma^{Q}(\hat{\varepsilon}, \boldsymbol{k})$ and $\sigma^{D}(\hat{\varepsilon})$ are real, one deduces the relation $\sigma(l, -m) = (-1)^{m}[\sigma(l, m)]^{*}$. Therefore, writing $\sigma(l, m) = \sigma^{r}(l, m) + i\sigma^{i}(l, m)$, one obtains

$$\sigma^{r}(l, -m) = (-1)^{m}\sigma^{r}(l, m) \quad \text{and} \quad \sigma^{i}(l, -m) = -(-1)^{m}\sigma^{i}(l, m). \tag{A11}$$

Appendix 2. Multiple-scattering calculation of the tensor components of the absorption cross section

This appendix presents a theoretical calculation of the angular-dependent dipole and quadrupole transitions. From the result of this calculation, it will be possible to derive a relationship between the experimental data $\sigma(l, m)$ and the scattering path operator which is the output of most multiple-scattering programs. The following results are derived in the one-electron spherical muffin-tin approximation.

Physically, the scattering path operator matrix element, $\tau^{ij}_{LL'} = \langle lm|\tau^{ij}|l'm'\rangle$ represents the sum of all contributions corresponding to scattering paths starting from a spherical wave $|lm\rangle$ at site i and ending as a spherical wave $|l'm'\rangle$ at site j. In other words, if a spherical wave $|lm\rangle$ is sent from site i, $\langle lm|\tau^{ij}|l'm'\rangle$ is the component $|l'm'\rangle$ of the response of the molecule or crystal at site j [170, 171].

The polarised absorption cross section in the dipole approximation has been calculated by the multiple-scattering approach in a number of cases [70, 137, 140, 141, 172–187, 255]. The following provides a relationship between the absorption cross-section tensor and the scattering path operators. The advantage of this relationship is that all the angle-resolved spectra can be calculated at the same time. The multiple-scattering programs give the matrix elements of the scattering path operators, from which the absorption cross-section tensor can be derived. The absorption cross section for a given polarisation direction can then be obtained by the appropriate linear combination (4.7).

To establish a relationship between the experimental parameters of the tensor expansion of the absorption spectra and the theoretical calculation we need to define the spherical tensor components of the scattering path operators by

$$\tau(l, l'; c, \gamma) \equiv \sum_{mm'} (-1)^{l+m}(lml'm'|c\gamma)\langle \kappa l - m|\tau^{00}|\kappa l'm'\rangle. \tag{A12}$$

An expansion of $\tau(l, l'; c, \gamma)$ in terms of single- and multiple-scattering contributions has been given in reference [98].

A2.1 Electric dipole transition

As shown in reference [98], the dipole contribution to the absorption cross section is

$$\sigma^{D}(\hat{\varepsilon}) = (4\pi)^2\alpha\hbar\omega\kappa^2(1/3)(2m/\hbar^2)(2l_0+1)\sum_{ll''} M^{D}_{l_0 l}M^{D}_{l_0 l''}(l_0 010|l0)(l_0 010|l''0)$$
$$\times \sum_{c\gamma} W(1l_0 cl''; l1)\langle c\|1\|1\rangle \operatorname{Im}\{\tau(l, l''; c, \gamma)Y^{\gamma *}_{c}(\hat{\varepsilon})\} \tag{A13}$$

where $M^{D}_{l_0 l} \equiv \int r^2\, \mathrm{d}r R_l(r) r R^{c}_{l_0}(r)$ is the atomic dipole reduced matrix element. Note that, for notational convenience, the factor $\sin(\delta^0_l)$ is not used here as in reference [98]. $R^{c}_{l_0}(r)Y^{m_0}_{l_0}(\hat{r})$ is the wavefunction of the core electron (before absorption) and $R_l(r)Y^{m}_{l}(\hat{r})$ is the photoelectron wavefunction inside the muffin-tin sphere. It is defined so that the radial part $R_l(r)$ matches $j_l(\kappa r)\cot(\delta^0_l) - n_l(\kappa r)$ smoothly at the muffin-tin radius of the photoabsorbing atom (δ^0_l is the lth phase shift of the photoabsorbing atom; the index 0 refers to the absorbing site). The other symbols are defined in section A2.2.

If we identify this expression with the formula giving the experimental tensor parameters (A4), we obtain

$$\sigma^{D}(c, \gamma) = -4\pi\alpha\hbar\omega\kappa^2(1/\sqrt{3})(2m/\hbar^2)(2l_0+1)\sum_{ll''} M^{D}_{l_0 l}M^{D}_{l_0 l''}(l_0 010|l0)(l_0 010|l''0)$$
$$\times W(1l_0 cl''; l1)(-\mathrm{i}/2)\{\tau(l, l''; c, \gamma) - (-1)^{\gamma}[\tau(l, l''; c, -\gamma)]^*\}. \tag{A14}$$

To be specific, we shall study the case of a K-edge. Then the angle-resolved absorption cross section reduces to:

$$\sigma^{D}(0, 0) = -4\pi/(3\sqrt{3})\alpha\hbar\omega\kappa^2(2m/\hbar^2)(M^{D}_{01})^2 \operatorname{Im}\{\tau(1, 1; 0, 0)\} \tag{A15}$$

$$\sigma^{D}(2, \gamma) = -4\pi/(3\sqrt{3})\alpha\hbar\omega\kappa^2(2m/\hbar^2)(M^{D}_{01})^2(-\mathrm{i}/2)$$
$$\times \{\tau(1, 1; 2, \gamma) - (-1)^{\gamma}[\tau(1, 1; 2, -\gamma)]^*\}. \tag{A16}$$

A2.2. Electric quadrupole transitions

The electric quadrupole absorption cross section is:

$$\sigma^{Q}(\hat{\varepsilon}, \boldsymbol{k}) = -\pi\alpha\hbar\omega\kappa^2 \operatorname{Im}\left(\sum_{m_0}\sum_{LL''} M^{Q*}_{L} M^{Q}_{L''}\langle\kappa L|\tau^{00}|\kappa L''\rangle\right)(2m/\hbar^2) \tag{A17}$$

where α is the fine structure constant, $\hbar\omega$ is the energy of the x-ray photon, κ is the photoelectron wavenumber, L is the compound index $L \equiv (l, m)$ and l_0 and m_0 are the azimuthal and magnetic quantum numbers of the core electrons in the initial state, respectively. Furthermore we have defined the atomic electric quadrupole matrix element: $M^{Q}_{L} \equiv \int \mathrm{d}^3 r R_l(r)Y^{m*}_{l}(\hat{r})\hat{\varepsilon}\cdot\boldsymbol{r}\boldsymbol{k}\cdot\boldsymbol{r}R^{c}_{l_0}(r)Y^{m_0}_{l_0}(\hat{r})$, with the same notation as for the electric dipole term.

Using

$$\hat{\varepsilon}\cdot\boldsymbol{r} = (4\pi/3)r\sum_{\lambda} Y^{\lambda *}_{1}(\hat{r})Y^{\lambda}_{1}(\hat{\varepsilon}) \tag{A18}$$

$$\boldsymbol{k}\cdot\boldsymbol{r} = (4\pi/3)kr\sum_{\mu} Y^{\mu *}_{1}(\hat{r})Y^{\mu}_{1}(\hat{k}) \tag{A19}$$

the atomic electric quadrupole matrix element can be written:

$$M_L^Q = (4\pi/3)^2 k M_{l_0 l}^Q \sum_{\lambda\mu} \int \mathrm{d}\Omega Y_l^{m*}(\hat{r}) Y_1^{\lambda *}(\hat{r}) Y_1^{\lambda}(\hat{\varepsilon}) Y_1^{\mu *}(\hat{r}) Y_1^{\mu}(\hat{k}) Y_{l_0}^{m_0}(\hat{r}) \tag{A20}$$

where $M_{l_0 l}^Q \equiv \int r^2 \,\mathrm{d}r R_l(r) r^2 R_{l_0}^c(r)$ integrates the radial parts of the wavefunctions. The product of spherical harmonics can be expanded (equation (3.436) of reference [36]):

$$Y_1^{\lambda *}(\hat{r}) Y_1^{\mu *}(\hat{r}) = \sum_{\nu} C_{1\lambda 1\mu}^{2\nu} Y_2^{\nu *}(\hat{r}) + C_{1\lambda 1\mu}^{00} Y_0^{0*}(\hat{r}) \tag{A21}$$

where $C_{1\lambda 1\mu}^{2\nu}$ is a Gaunt coefficient (see A26).

First, consider the second term of this sum. On introducing it into the quadrupole matrix element we obtain:

$$\sum_{\lambda\mu} C_{1\lambda 1\mu}^{00} \int \mathrm{d}\Omega Y_l^{m*}(\hat{r}) Y_0^{0*}(\hat{r}) Y_1^{\lambda}(\hat{\varepsilon}) Y_1^{\mu}(\hat{k}) Y_{l_0}^{m_0}(\hat{r})$$

$$= (1/4\pi) \sum_{\lambda} Y_1^{\lambda *}(\hat{\varepsilon}) Y_1^{\lambda}(\hat{k}) \delta_{l l_0} \delta_{m m_0} = 3/(4\pi)^2 P_1(\hat{k}\cdot\hat{\varepsilon}) \delta_{l l_0} \delta_{m m_0} = 0 \tag{A22}$$

since the Legendre polynomial $P_1(\hat{k}\cdot\hat{\varepsilon}) = \hat{k}\cdot\hat{\varepsilon} = 0$. Therefore, we obtain:

$$M_L^Q = (4\pi/3)^2 k M_{l_0 l}^Q \sum_{\lambda\mu\nu} C_{l m 2\nu}^{l_0 m_0} C_{1\lambda 1\mu}^{2\nu} Y_1^{\lambda}(\hat{\varepsilon}) Y_1^{\mu}(\hat{k}) \tag{A23}$$

and the quadrupole absorption cross section becomes

$$\sigma^Q(\hat{\varepsilon}, \boldsymbol{k}) = -\pi\alpha\hbar\omega\kappa^2 (2m/\hbar^2)(4\pi/3)^4 k^2 \sum_{l l'} M_{l_0 l}^Q M_{l_0 l'}^Q$$

$$\times \mathrm{Im}\Bigg(\sum_{\nu\nu'} \sum_{\lambda\lambda'} \sum_{\mu\mu'} C_{1\lambda 1\mu}^{2\nu} C_{1\lambda' 1\mu'}^{2\nu'} Y_1^{\lambda *}(\hat{\varepsilon}) Y_1^{\mu *}(\hat{k}) Y_1^{\lambda'}(\hat{\varepsilon}) Y_1^{\mu'}(\hat{k})$$

$$\times \sum_{m_0} \sum_{m m'} C_{l m 2\nu}^{l_0 m_0} C_{l' m' 2\nu}^{l_0 m_0} \langle \kappa l m | \tau^{00} | \kappa l' m' \rangle \Bigg). \tag{A24}$$

The above expression will be simplified in three steps.

(i) The last sum (over m_0, m and m') can be evaluated by using the expansion of the scattering path operators over spherical tensors [98]:

$$\langle \kappa l m | \tau^{00} | \kappa l' m' \rangle = \sum_{c\gamma} \tau(l, l'; c, \gamma)(-1)^{l-m} (l\ -m\, l' m' | c\gamma). \tag{A25}$$

Following equation (3.437) of reference [36] we define the reduced matrix element:

$$\langle a \| b \| c \rangle \equiv \{(2b+1)(2c+1)/[4\pi(2a+1)]\}^{1/2} (b0c0|a0)$$

so that the Gaunt coefficients can be written

$$C_{b\beta c\gamma}^{a\alpha} = \langle a \| b \| c \rangle (b\beta c\gamma | a\alpha). \tag{A26}$$

Using this notation, the identity (3.269) of reference [36]

$$\sum_{m'} (lma\alpha | l'm')(l'm'b\beta | l''m'')$$

$$= \sum_{c\gamma} [(2l'+1)(2c+1)]^{1/2} W(lal''b; l'c)(a\alpha b\beta | c\gamma)(lmc\gamma | l''m'') \tag{A27}$$

and the orthogonality of the Clebsch–Gordan coefficients we find:

$$\sum_{m_0}\sum_{mm'} C^{l_0 m_0}_{lm2\nu} C^{l_0 m_0}_{l'm'2\nu'} \langle \kappa l m|\tau^{00}|\kappa l' m'\rangle = \langle l_0\|l\|2\rangle\langle l_0\|l'\|2\rangle \times \sum_{c\gamma} \tau(l,l';c,\gamma)(2l_0+1)W(2l_0 cl';l2)(-1)^{\nu'}(2\nu 2-\nu'|c\gamma). \tag{A28}$$

when $W(2l_0cl';l2)$ is a Racah coefficient [36].

(ii) To calculate the intermediate sum (over λ, λ', μ and μ'), we first write

$$Y_1^{\lambda *}(\hat{\varepsilon})Y_1^{\lambda'}(\hat{\varepsilon}) = \sum_{a\alpha} C^{1\lambda}_{1\lambda' a\alpha} Y_a^{\alpha *}(\hat{\varepsilon}) \tag{A29}$$

$$Y_1^{\mu *}(\hat{k})Y_1^{\mu'}(\hat{k}) = \sum_{b\beta} C^{1\mu}_{1\mu' b\beta} Y_b^{\beta *}(\hat{k}). \tag{A30}$$

Then one uses the coupling formula (A27), with dummy indices (d, δ), to carry out the sum over λ and μ', next the orthogonality relation for the sum over λ' and μ, and finally the coupling formula again for the sum over the dummy index δ to obtain

$$\begin{aligned}\sum_{\lambda\lambda'}\sum_{\mu\mu'} C^{2\nu}_{1\lambda 1\mu} C^{2\nu'}_{1\lambda' 1\mu'} Y_1^{\lambda *}(\hat{\varepsilon})Y_1^{\mu *}(\hat{k})Y_1^{\lambda'}(\hat{\varepsilon})Y_1^{\mu'}(\hat{k}) &= \langle 2\|1\|1\rangle^2 \sum_{ab}\langle 1\|1\|a\rangle\langle 1\|1\|b\rangle \sum_{\alpha\beta} Y_a^{\alpha *}(\hat{\varepsilon})Y_b^{\beta *}(\hat{k}) \\ &\times \sum_{d'\delta'}\sum_{d} 15(2d+1)[(2d'+1)/(2a+1)]^{1/2}(-1)^{\beta+\nu'} \\ &\times W(a121;1d)W(21b1;1d)W(b2a2;dd') \\ &\times (2-\nu' 2\nu|d'\delta')(b-\beta d'\delta'|a\alpha).\end{aligned} \tag{A31}$$

(iii) The first sum (over ν and ν') is now completed by using the orthogonality of the Clebsch–Gordan coefficients. This gives:

$$\begin{aligned}\sigma^{Q}(\hat{\varepsilon},\boldsymbol{k}) = &-\pi\alpha\hbar\omega\kappa^2(2m/\hbar^2)(4\pi/3)^4 k^2(2l_0+1)\langle 2\|1\|1\rangle^2 \\ &\times \sum_{ll'} M^{Q}_{l_0 l} M^{Q}_{l_0 l'} \langle l_0\|l\|2\rangle\langle l_0\|l'\|2\rangle \sum_{c} W(2l_0 cl';l2) \\ &\times \sum_{ab}\langle 1\|1\|a\rangle\langle 1\|1\|b\rangle 15 \sum_{d}(2d+1)W(a121;1d)W(b121;1d) \\ &\times W(a2b2;dc)\,\mathrm{Im}\left(\sum_{\alpha\beta\gamma}(a\alpha b\beta|c\gamma)Y_a^{\alpha *}(\hat{\varepsilon})Y_b^{\beta *}(\hat{k})\tau(l,l';c,\gamma)\right).\end{aligned} \tag{A32}$$

The above expression may seem complicated, but it can be made more explicit by noticing that, because of the selection rule included in $\langle 1\|1\|a\rangle$, a and b are 0 or 2. Secondly, the initial expression (A6) for $\sigma^{Q}(\hat{\varepsilon},\boldsymbol{k})$ is symmetric in $\hat{\varepsilon}$ and $\hat{k}$. If we interchange $\hat{\varepsilon}$ and $\hat{k}$ in (A32), then interchange $(a\alpha)$ and $(b\beta)$ in the sums, we must use $(a\alpha b\beta|c\gamma) = (-1)^{a+b+c}(b\beta a\alpha|c\gamma)$ to obtain the same expression. Since a and b are even, the equality of the two expressions before and after the interchanges shows that no term in which c is odd contributes to the sum. This, together with the triangle condition on $(a\alpha b\beta|c\gamma)$ proves that c can only take the values 0, 2 and 4. Therefore, if we call

$$B(a,b,c) \equiv 15\sum_{ab}\langle 1\|1\|a\rangle\langle 1\|1\|b\rangle\sum_{d}(2d+1)W(a121;1d)W(b121;1d)W(a2b2;dc) \tag{A33}$$

we can compute the only terms that contribute to the cross section once and for all:

$$B(0,0,0) = \sqrt{5}/4\pi \qquad B(2,0,2) = B(0,2,2) = -(1/4\pi)\sqrt{7/10}$$
$$B(2,2,0) = 1/20\pi \qquad B(2,2,2) = -1/20\pi \qquad B(2,2,4) = 3/10\pi. \tag{A34}$$

For a K-edge this yields

$$\sigma^{Q}(\hat{\varepsilon}, \boldsymbol{k}) = -\pi\alpha\hbar\omega\kappa^2(2m/\hbar^2)(4\pi/3)^3k^2(1/10)(M^{Q}_{02})^2 \times \sum_{abc} B(a,b,c)\,\mathrm{Im}\left(\sum_{\alpha\beta\gamma}(a\alpha b\beta|c\gamma)Y^{\alpha}_{a}{}^{*}(\hat{\varepsilon})Y^{\beta *}_{b}(\hat{k})\tau(2,2;c,\gamma)\right). \tag{A35}$$

If we identify the general result (A32) with the definition of the experimental parameters of the tensor expansion of the electric quadrupole contribution to the absorption cross section (A7) we obtain

$$\sigma^{Q}(c,\gamma) = -\pi\alpha\hbar\omega\kappa^2(2m/\hbar^2)4\pi/(15\sqrt{5})k^2(2l_0+1)\langle 2\|1\|1\rangle^2 \times \sum_{ll'} M^{Q}_{l_0l}M^{Q}_{l_0l'}\langle l_0\|l\|2\rangle\langle l_0\|l'\|2\rangle W(2l_0cl';l2)(-\mathrm{i}/2)\{\tau(l,l';c,\gamma) - (-)^{\gamma}[\tau(l,l';c,-\gamma)]^{*}\}. \tag{A36}$$

If one averages the above result over polarisation and wavevector directions (taking into account the fact that these two vectors are orthogonal), one obtains the quadrupole absorption cross section for unoriented samples:

$$\langle\sigma^{Q}\rangle = -\pi\alpha\hbar\omega\kappa^2(2m/\hbar^2)k^2(1/15) \times \sum_{l}(M^{Q}_{l_0l})^2\sqrt{2l+1}\,(l020|l_00)^2\,\mathrm{Im}\{\tau(l,l;0,0)\}. \tag{A37}$$

It can be checked that, as expected, $\langle\sigma^{Q}\rangle = \sigma^{Q}(0,0)$.

Appendix 3. General formulae for samples without symmetry

A3.1. Angular dependence of the quadrupole contribution to the absorption cross section

The most general angular dependence of the quadrupole contribution to the absorption cross section contains 15 parameters, the experimental determination of which would be extremely difficult. However, for completeness and theoretical applications, this appendix is devoted to the general expression:

$$\begin{aligned}\sigma^{Q}(\hat{\varepsilon},\hat{k}) = {} & \sigma^{Q}(0,0) + \sqrt{5/14}\,(3\sin^2\theta\sin^2\psi - 1)\sigma^{Q}(2,0) \\ & + 2\sqrt{15/7}\sin\theta\sin\psi[\cos\theta\sin\psi(\sigma^{Qr}(2,1)\cos\varphi + \sigma^{Qi}(2,1)\sin\varphi) \\ & + \cos\psi(\sigma^{Qr}(2,1)\sin\varphi - \sigma^{Qi}(2,1)\cos\varphi)] \\ & + \sqrt{15/7}\,[(\cos^2\theta\sin^2\psi - \cos^2\psi)(\sigma^{Qr}(2,2)\cos(2\varphi) + \sigma^{Qi}(2,2)\sin(2\varphi)) \\ & + 2\cos\theta\sin\psi\cos\psi(\sigma^{Qr}(2,2)\sin(2\varphi) - \sigma^{Qi}(2,2)\cos(2\varphi))] \\ & + 1/\sqrt{14}\,[35\sin^2\theta\cos^2\theta\cos^2\psi + 5\sin^2\theta\sin^2\psi - 4]\sigma^{Q}(4,0) \\ & + \sqrt{10/7}\sin\theta[(14\cos^2\theta\cos^2\psi + 8\sin^2\psi - 7)\cos\theta(\sigma^{Qr}(4,1) \\ & \times\cos\varphi + \sigma^{Qi}(4,1)\sin\varphi) - (7\cos^2\theta - 1)\sin\psi\cos\psi(\sigma^{Qr}(4,1) \\ & \times\sin\varphi - \sigma^{Qi}(4,1)\cos\varphi)] - 2\sqrt{5/7}\,[(7\sin^2\theta\cos^2\theta\cos^2\psi\end{aligned}$$

$$+ \cos^2\theta \sin^2\psi - \cos^2\psi)(\sigma^{Qr}(4,2)\cos(2\varphi) + \sigma^{Qi}(4,2)\sin(2\varphi))$$
$$- (7\sin^2\theta - 2)\cos\theta \sin\psi \cos\psi(\sigma^{Qr}(4,2)\sin(2\varphi)$$
$$- \sigma^{Qi}(4,2)\cos(2\varphi))] + \sqrt{10}\sin\theta[(1 - 2\cos^2\theta\cos^2\psi)$$
$$\times \cos\theta(\sigma^{Qr}(4,3)\cos(3\varphi) + \sigma^{Qi}(4,3)\sin(3\varphi))$$
$$+ (3\cos^2\theta - 1)\sin\psi\cos\psi(\sigma^{Qr}(4,3)\sin(3\varphi) - \sigma^{Qi}(4,3)\cos(3\varphi))]$$
$$+ \sqrt{5}\sin^2\theta[(\cos^2\theta\cos^2\psi - \sin^2\psi)(\sigma^{Qr}(4,4)\cos(4\varphi)$$
$$+ \sigma^{Qi}(4,4)\sin(4\varphi)) - 2\cos\theta\sin\psi\cos\psi(\sigma^{Qr}(4,4)\sin(4\varphi)$$
$$- \sigma^{Qi}(4,4)\cos(4\varphi))]. \tag{A38}$$

A3.2. Dipole absorption matrix elements

In §7.1, a dipole absorption matrix $\boldsymbol{\sigma}^{D}$ was defined to calculate the response of a sample to an x-ray beam with general polarisation. In this appendix, the matrix elements of this matrix are given. The incident x-ray wavevector is that of §7.1. Formulae (A39*a*)–(A39*c*) are for a sample without symmetry. To take the symmetry of the crystal into account, keep only the non-zero tensor components $\sigma^{D}(l, m)$ of the corresponding point-symmetry group, as in §4:

$$\sigma^{Dxx} = \sigma^{D}(0,0) - 1/\sqrt{2}\,(3\sin^2 2\theta - 1)\sigma^{D}(2,0) - \sqrt{3}\sin(\theta)$$
$$\times (\cos\varphi\sigma^{Dr}(2,1) + \sin\varphi\sigma^{Di}(2,1)) - \sqrt{3}\cos^2\theta(\cos(2\varphi)\sigma^{Dr}(2,2)$$
$$+ \sin(2\varphi)\sigma^{Di}(2,2)) \tag{A39a}$$

$$\sigma^{Dxy} = \sigma^{Dyx} = \sqrt{3}\sin\theta(\sin\varphi\sigma^{Dr}(2,1) - \cos\varphi\sigma^{Di}(2,1))$$
$$+ \sqrt{3}\cos\theta(\sin(2\varphi)\sigma^{Dr}(2,2) - \cos(2\varphi)\sigma^{Di}(2,2)) \tag{A39b}$$

$$\sigma^{Dyy} = \sigma^{D}(0,0) + 1/\sqrt{2}\,\sigma^{D}(2,0) + \sqrt{3}\,(\cos(2\varphi)\sigma^{Dr}(2,2) + \sin(2\varphi)\sigma^{Di}(2,2)). \tag{A39c}$$

A3.3. Quadrupole absorption matrix elements

This appendix gives the matrix elements of σ^{Q}. The incident x-ray wavevector is defined in §7.1. Formulae (A40*a*)–(A40*c*) are for a sample without symmetry. To take the symmetry of the crystal into account, keep only the non-zero tensor components $\sigma^{Q}(l, m)$ of the corresponding point symmetry group, as in §5:

$$\sigma^{Qxx} = \sigma^{Q}(0,0) - \sqrt{5/14}\sigma^{Q}(2,0) - \sqrt{15/7}\,(\sigma^{Qr}(2,2)\cos(2\varphi) + \sigma^{Qi}(2,2)\sin(2\varphi))$$
$$+ 1/\sqrt{14}(35\sin^2\theta\cos^2\theta - 4)\sigma^{Q}(4,0)$$
$$+ \sqrt{35/2}\sin(2\theta)\cos(2\theta)(\sigma^{Qr}(4,1)\cos\varphi + \sigma^{Qi}(4,1)\sin\varphi)$$
$$- 2\sqrt{5/7}[(7\sin^2\theta\cos^2\theta - 1)(\sigma^{Qr}(4,2)\cos(2\varphi) + \sigma^{Qi}(4,2)\sin(2\varphi))$$
$$- \sqrt{5/2}\sin(2\theta)\cos(2\theta)(\sigma^{Qr}(4,3)\cos(3\varphi) + \sigma^{Qi}(4,3)\sin(3\varphi))$$
$$+ \sqrt{5}\sin^2\theta\cos^2\theta(\sigma^{Qr}(4,4)\cos(4\varphi) + \sigma^{Qi}(4,4)\sin(4\varphi)) \tag{A40a}$$

$$\sigma^{Qxy} = \sigma^{Qyx} = \sqrt{15/7}\sin\theta(\sigma^{Qr}(2,1)\sin\varphi - \sigma^{Qi}(2,1)\cos\varphi)$$
$$+ \sqrt{15/7}\cos\theta(\sigma^{Qr}(2,2)\sin(2\varphi) - \sigma^{Qi}(2,2)\cos(2\varphi))$$
$$- \sqrt{5/14}\sin\theta(7\cos^2\theta - 1)(\sigma^{Qr}(4,1)\sin\varphi - \sigma^{Qi}(4,1)\cos\varphi)$$
$$+ \sqrt{5/7}\cos\theta(7\sin^2\theta - 2)(\sigma^{Qr}(4,2)\sin(2\varphi) - \sigma^{Qi}(4,2)\cos(2\varphi))$$
$$+ \sqrt{5/2}\sin\theta(3\cos^2\theta - 1)(\sigma^{Qr}(4,3)\sin(3\varphi) - \sigma^{Qi}(4,3)\cos(3\varphi))$$
$$- \sqrt{5}\cos\theta\sin^2\theta(\sigma^{Qr}(4,4)\sin(4\varphi) - \sigma^{Qi}(4,4)\cos(4\varphi)) \qquad (A40b)$$

$$\sigma^{Qyy} = \sigma^{Q}(0,0) + \sqrt{5/14}\,(3\sin^2\theta - 1)\sigma^{Q}(2,0)$$
$$+ \sqrt{15/7}\sin(2\theta)(\sigma^{Qr}(2,1)\cos\varphi + \sigma^{Qi}(2,1)\sin\varphi)$$
$$+ \sqrt{15/7}\cos^2\theta(\sigma^{Qr}(2,2)\cos(2\varphi)$$
$$+ \sigma^{Qi}(2,2)\sin(2\varphi)) - 1/\sqrt{14}\,(5\cos^2\theta - 1)\,\sigma^{Q}(4,0)$$
$$+ \sqrt{5/14}\sin(2\theta)(\sigma^{Qr}(4,1)\cos\varphi + \sigma^{Qi}(4,1)\sin\varphi)$$
$$- 2\sqrt{5/7}\cos^2\theta(\sigma^{Qr}(4,2)\cos(2\varphi) + \sigma^{Qi}(4,2)\sin(2\varphi))$$
$$+ \sqrt{5/2}\sin(2\theta)(\sigma^{Qr}(4,3)\cos(3\varphi) + \sigma^{Qi}(4,3)\sin(3\varphi))$$
$$- \sqrt{5}\sin^2\theta(\sigma^{Qr}(4,4)\cos(4\varphi) + \sigma^{Qi}(4,4)\sin(4\varphi)). \qquad (A40c)$$

Appendix 4. Useful Clebsch–Gordan coefficients

Since the Clebsch–Gordon coefficients used satisfy the symmetry relations $(lml'm'|l''m'') = (l - ml' - m'|l'' - m'') = (l'm'lm|l''m'')$, the following list is sufficient for translating the molecular-orbital picture into the x-ray absorption tensor components and vice versa:

$(1010|00) = -1/\sqrt{3}$ $(111-1|00) = 1/\sqrt{3}$ $(1010|20) = \sqrt{2/3}$
$(111-1|20) = 1/\sqrt{6}$ $(1011|21) = 1/\sqrt{2}$ $(1111|22) = 1$
$(2020|00) = 1/\sqrt{5}$ $(212-1|00) = -1/\sqrt{5}$ $(222-2|00) = 1/\sqrt{5}$
$(2020|20) = -\sqrt{2/7}$ $(212-1|20) = 1/\sqrt{14}$ $(222-2|20) = \sqrt{2/7}$
$(2021|21) = -1/\sqrt{14}$ $(222-1|21) = \sqrt{3/7}$ $(2022|22) = \sqrt{2/7}$
$(2121|22) = -\sqrt{3/7}$ $(2020|40) = 3\sqrt{2/35}$ $(212-1|40) = 2\sqrt{2/35}$
$(222-2|40) = \sqrt{1/70}$ $(2021|41) = \sqrt{3/7}$ $(222-1|41) = 1/\sqrt{14}$
$(2022|42) = \sqrt{3/14}$ $(2121|42) = 2/\sqrt{7}$ $(2122|43) = 1/\sqrt{2}$
$(2222|44) = 1$

References

[1] Kronig R 1932 *Z. Phys.* **75** 191–210
[2] Cooksey C D and Stephenson S T 1933 *Phys. Rev.* **43** 670–1
[3] Stephenson S T 1933 *Phys. Rev.* **44** 349–52
[4] Hellwege K H 1948 *Ann. Phys., Lpz.* Ser. VI **4** 95–160
[5] Hellwege K H 1951 *Z. Phys.* **129** 626–41

[6] Hellwege K H 1951 *Z. Phys.* **131** 98–112
[7] Krogstad R, Nelson W and Stephenson S T 1953 *Phys. Rev.* **92** 1394–6
[8] El-Hussain J M and Stephenson S T 1958 *Phys. Rev.* **109** 51–4
[9] Singh J N 1961 *Phys. Rev.* **123** 1724–9
[10] Boster T A and Edwards J E 1962 *J. Chem. Phys.* **36** 3031–3
[11] Alexander E, Fraenkel B S, Perel J and Rabinovitch K 1963 *Phys. Rev.* **132** 1554–9
[12] Calas G and Petiau J 1983 *Solid State Commun.* **48** 625–9
[13] Grunes L A 1983 *Phys. Rev.* B **27** 2111–31
[14] Poumellec B, Marucco J F and Touzelin B 1987 *Phys. Rev.* B **35** 2284–94
[15] Shulman R G, Yafet Y, Eisenberger P and Blumberg W E 1976 *Proc. Nat. Acad. Sci.* **73** 1384–8
[16] Wong J, Lytle F W, Messmer R P and Maylotte D H 1984 *Phys. Rev.* B **30** 5596–610
[17] Brümmer O, Dräger G and Starke W 1971 *J. Physique Coll.* **10** C4 169–71
[18] Heald S M and Stern E A 1977 *Phys. Rev.* B **16** 5549–59
[19] Goulon J, Goulon-Ginet C, Cortes R and Dubois J M 1982 *J. Physique* **43** 539–48
[20] Stöhr J 1988 *X-ray Absorption. Principles, applications, techniques of EXAFS, SEXAFS and XANES* ed. D C Koningsberger and R Prins (New York: Wiley) pp 443–571
[21] Oyanagi H, Tokumoto M, Ishiguro T, Shirakawa H, Nemoto H, Matsushita T, Ito M and Kuroda H 1984 *J. Phys. Soc. Japan* **53** 4044–53
[22] Landau L D and Lifshitz E M 1977 *Quantum Mechanics* (Oxford: Pergamon)
[23] Bethe H A and Salpeter E E 1977 *Quantum Mechanics of One- and Two-Electron Atoms* (New York: Plenum) §66 and p 252
[24] Blinder S M 1974 *Foundations of Quantum Dynamics* (London: Academic) p 205
[25] Cowan R D 1981 *The Theory of Atomic Structure and Spectra* (Berkeley, CA: University of California Press) ch 15
[26] Pagel B E J 1969 *Mém. Soc. Roy. Sci. Liège* **17** 189–205
[27] Ekberg J O, Seely J F, Brown C M, Feldman U, Richardson M C and Behring W E 1987 *J. Opt. Soc. Am.* B **4** 420–3
[28] Lucchese R R, Takatsuka K and McKoy V 1986 *Phys. Rep.* **131** 147–221
[29] Green T A 1985 *Phys. Rev.* B **32** 3442–5
[30] Soff G and Müller B 1977 *Z. Phys.* A **280** 243–7
[31] Briand J P 1983 *Fundamental Processes in Energetic Atomic Collisions* ed. H O Lutz, J S Briggs and H Kleinpoppin (New York: Plenum) pp 183–252
[32] Edlabadkar V S and Mande C 1982 *J. Phys. B: At. Mol. Phys.* **15** 2339–48
[33] Robinson J W (ed.) 1974 *Handbook of Spectroscopy* vol I (Cleveland, OH: CRC) p 119
[34] Wagenfeld H 1966 *Phys. Rev.* **144** 216–24
[35] Hildebrandt G, Stephenson J D and Wagenfeld H 1973 *Z. Naturf.* a **28** 588–600
[36] Biedenharn L C and Louck J D 1981 *Angular Momentum in Quantum Physics* (Reading, MA: Addison-Wesley) ch 3
[37] Born M and Wolf E 1980 *Principles of Optics* 6th edn (Oxford: Pergamon) p 711 and §108
[38] Templeton D H and Templeton L K 1980 *Acta Crystallogr.* A **36** 237–41
[39] Templeton D H and Templeton L K 1982 *Acta Crystallogr.* A **38** 62–7
[40] Templeton D H and Templeton L K 1985 *Acta Crystallogr.* A **41** 133–42
[41] Templeton D H and Templeton L K 1985 *Acta Crystallogr.* A **41** 365–71
[42] Templeton D H and Templeton L K 1989 *Acta Crystallogr.* A **45** 39–42
[43] Dmitrienko V E 1983 *Acta Crystallogr.* A **39** 29–35
[44] Petcov A, Kirfel A and Fischer K 1988 *Z. Naturf.* a **43** 388–90
[45] Bonse U and Henning A 1986 *Nucl. Instrum. Methods Phys. Res.* A **246** 814–6
[46] Kostarev A I 1965 *Phys. Met. Metallogr.* **19** 1–9
[47] Kostarev A I 1965 *Phys. Met. Metallogr.* **20** 25–30 (Erratum 1966 **22** 166–7)
[48] Kostarev A I 1967 *Opt. Spectrosc.* **22** 163–5
[49] Kostarev A I and Weber W M 1971 *Phys. Rev.* B **3** 4124–33
[50] Izraileva L K 1966 *Sov. Phys.–Dokl.* **11** 506–8
[51] Perel J 1966 *Phys. Rev.* **147** 463–6
[52] Izraileva L K 1967 *Sov. Phys.–Dokl.* **11** 709–11
Izraileva L K 1969 *X-ray Spectra and Electronic Structure of Matter* vol II (Kiev: Inst. Metallofiz. Akad. Nauk. pp 211–221 (in Russian)
Izraileva L K 1970 *PhD Thesis* Rostov-on-Don pp 1–19 (in Russian)
[53] Weber W M 1972 *PhD Thesis*, Groningen University

[54] Schaich W L 1973 *Phys. Rev.* B **8** 4028–32
[55] Stern E A 1974 *Phys. Rev.* B **10** 3027–37
[56] Keilacker H and Meisel A 1974 *Ann. Phys., Lpz.* Ser. VII **31** 239–46
[57] Brown G S, Eisenberger P and Schmidt P 1977 *Solid State Commun.* **24** 201–3
[58] Rabe P, Tolkiehn G and Werner A 1980 *J. Phys. C: Solid State Phys.* **13** 1857–64
[59] Cox A D and Beaumont J H 1980 *Phil. Mag.* B **42** 115–26
[60] Döbler U, Baberschke K, Haase J and Puschmann A 1984 *Phys. Rev. Lett.* **52** 1437–40
[61] Oyanagi H, Sugi M, Kuroda S, Iizima S, Ishiguro T and Matsushita T 1985 *Thin Solid Films* **133** 181–8
[62] Tokumoto M, Oyanagi H, Ishiguro T, Shirakawa H, Nemoto H, Matsushita T and Kuroda H 1985 *Mol. Cryst. Liq. Cryst.* **17** 139–46
[63] Feldman J L, Elam W T, Ehrlich A C, Skelton E F, Dominguez D D, Chung D D L and Lytle F W 1986 *Phys. Rev.* B **33** 7961–82
[64] Feldman J L, Skelton E F, Ehrlich A C, Dominguez D D, Elam W T, Qadri S B and Lytle F W 1984 *Solid State Commun.* **49** 1023–5
[65] Krone W, Wortmann G, Frank K H, Kaindl G, Menke K and Roth S 1984 *Solid State Commun.* **52** 253–6
[66] McCrary V R, Sette F, Chen C T, Lovinger A J, Robin M B, Stöhr J and Zeigler J M 1988 *J. Chem. Phys.* **88** 5925–33
[67] Oyanagi H, Tokumoto M, Ishiguro T, Shirakawa H, Nemoto H, Matsushita T and Kuroda H 1984 *EXAFS and Near Edge Structure III* ed. K O Hodgson, B Hedman and J E Penner-Hahn (Berlin: Springer) pp 397–9
[68] Oyanagi H, Tokumoto M, Ishiguro T, Shirakawa H, Nemoto H, Matsushita T and Kuroda H 1986 *J. Physique Coll.* **47** C8 615–8
[69] Scott R A, Hahn J E, Doniach S, Freeman H C and Hodgson K O 1982 *J. Am. Chem. Soc.* **104** 5364–9
[70] Stizza S, Benfatto M, Bianconi A, Garcia J, Mancini G and Natoli C R 1986 *J. Physique Coll.* **47** C8 691–6
[71] Dartyge E and Sadoc A 1986 *J. Physique Coll.* **47** C8 1085–8
[72] Flank A M, Weininger M, Mortenson L E and Cramer S P 1986 *J. Am. Chem. Soc.* **108** 1049–55
[73] Hitchcock A P, Garrett J D and Tyliszczak T 1986 *J. Physique Coll.* **47** C8 1081–4
[74] Oyanagi H, Tokumoto M, Ishiguro T, Shirakawa H, Nemoto H, Matsushita T and Kuroda H 1987 *Synth. Met.* **17** 491–6
[75] Gädeke W, Koch E E, Dräger G, Frahm R and Saile V 1988 *Chem. Phys.* **124** 113–9
[76] Manceau A, Bonnin D, Kaiser P and Frétigny C 1988 *Phys. Chem. Minerals* **16** 180–5
[77] Maeyama S, Satow Y, Oshima M and Katsui A 1988 *Japan. J. Appl. Phys.* **27** L1657–60
[78] Maeyama S, Satow Y, Oshima M and Katsui A 1989 *Physica* B **158** 473–4
[79] Yang C Y, Heald S M, Tranquada J M, Moodenbaugh A R and Xu Youwen 1988 *Phys. Rev.* B **38** 6568–74
[80] MacDowell A A, Norman D and West J B 1986 *Rev. Sci. Instrum.* **57** 2667–79
[81] George G N, Prince R C, Frey T G and Cramer S P 1989 *Physica* B **158** 81–3
[82] Penner-Hahn J E 1984 *Stanford Synchrotron Radiation Laboratory Report* 84/03
[83] Piacentini M 1983 *Proc. Int. Conf. on EXAFS and Near Edge Structure, Frascati (Italy) 13–17 September 1982* ed. A Bianconi, L Incoccia and S Stipcich (Berlin: Springer) pp193–9
[84] Heald S M and Stern E A 1978 *Phys. Rev.* B **17** 4069–81
[85] Krone W, Wortmann G, Kaindl G and Schlögl R 1987 *Proc. NATO Advanced Study Institute on Chemical Physics of Intercalation, Castera Verduzan (France) 10–19 June 1987* (New York: Plenum) pp 371–4
[86] Wortmann G 1988 *Proc. Int. Colloq. on Layered Compounds, Pont-à-Mousson (France) 8–10 March 1988* ed. D Guérard and P Lagrange, pp 357–64
[87] Wortmann G, Krone W, Kaindl G and Schlögl R 1988 *Synth. Met.* **23** 139–45
[88] Wortmann G, Krone W and Kaindl G 1989 *Physica* B **158** 535–6
[89] Bonnin D and Kaiser P 1987 *Proc. NATO Advanced Study Institute on Chemical Physics of Intercalation, Castera Verduzan (France), 10–19 June, 1987* (New York: Plenum) pp 319–29
[90] Bonnin D, Bouat J, Kaiser P, Frétigny C and Béguin F 1986 *J. Physique Coll.* **47** C8 865–8
[91] George G N, Cramer S P, Frey T G and Prince R C 1987 *Advances in Membrane Biochemistry and Bioenergetics* ed. C H Kim, H Tedeschi, J J Diwan and J C Salerno (New York: Plenum) pp 429–38
[92] Hitchcock A P and Tyliszczak T 1987 *J. Phys. C: Solid State Phys.* **20** 981–92
[93] Thulke W, Haensel R and Rabe P 1983 *Phys. Status Solidi* a **78** 539–45
[94] Rossi G, Jin X, Santaniello A, DePadova P and Chandesris D 1989 *Phys. Rev. Lett.* **62** 191–4
[95] Stöhr J and Jaeger R 1983 *Phys. Rev.* B **27** 5146–9

[96] Barton J J and Shirley D A 1985 *Phys. Rev.* B **32** 1892–905
[97] Rennert P and Van Hung N 1988 *Phys. Status Solidi* b **148** 49–61
[98] Brouder C, Ruiz López M F, Pettifer R F, Benfatto M and Natoli C R 1989 *Phys. Rev.* B **39** 1488–500
[99] Benfatto M, Natoli C R, Brouder C, Pettifer R F and Ruiz López M F 1989 *Phys. Rev.* B **39** 1936–9
[100] Henry N F M and Lonsdale K 1965 *International Tables for X-ray Crystallography* vol I (Birmingham, UK: Kynoch)
[101] Wallace S and Dill D 1978 *Phys. Rev.* B **17** 1692–9
[102] Stöhr J and Jaeger R 1982 *Phys. Rev.* B **26** 4111–31
[103] Antonangeli F, Piacentini M, Girlanda R, Martino G and Giuliano E S 1985 *Phys. Rev.* B **32** 6644–9
[104] Loupias G, Chomilier J, Tarbes J, Ascone I, Goulon J, Guerard D and Elalem N 1986 *J. Physique Coll.* **47** C8 891–5
[105] Rosenberg R A, Love P J and Rehn V 1984 *EXAFS and Near Edge Structure III* ed. K O Hodgson, B Hedman and J E Penner-Hahn (Berlin: Springer) pp 70–2
[106] Rosenberg R A, Love P J and Rehn V 1986 *Phys. Rev.* B **33** 4034–7
[107] Outka D A, Stöhr J, Rabe J P, Swalen J D and Rotermund H H 1987 *Phys. Rev. Lett.* **59** 1321–4
[108] Tourillon G, Dartyge E, Fontaine A, Garrett R, Sagurton M, Xu P and Williams G P 1987 *Europhys. Lett.* **4** 1391–6
[109] Lindner T, Somers J, Bradshaw A M, Kilcoyne A L D and Woodruff D P 1988 *Surf. Sci.* **203** 333–52
[110] Himpsel F J, Chandrashekhar G V, McLean A B and Shafer M W 1988 *Phys. Rev.* B **38** 11946–8
[111] Outka D A, Stöhr J, Rabe J P and Swalen J D 1988 *J. Chem. Phys.* **88** 4076–87
[112] Pettifer R F, Brouder C, Benfatto M, Natoli C R, Hermes C and Ruiz López M F 1989 *Phys. Rev. B* submitted
[113] Frétigny C, Bonnin D and Cortès R 1986 *J. Physique Coll.* **47** C8 869–73
[114] Loupias G, Rabii S, Nozières S and Tatar R C 1989 *Phys. Rev. B* at press
[115] Vvedensky D D, Salkin D K and Pendry J B 1985 *Surf. Sci.* **162** 909–12
[116] Cherkashenko V M, Dolgikh V E and Volkov V L 1988 *Sov. Phys.–Solid State* **30** 220–2
[117] Parkin S S P and Acrivos J V 1983 *J. Physique Coll.* **44** C3 1011–5
[118] Lindner T and Somers J 1988 *Phys. Rev.* B **37** 10039–44
[119] Rubinowicz A 1930 *Z. Phys.* **61** 338–48
[120] Rubinowicz A und Blaton J 1932 *Ergebnisse der exakten Naturwissenschaften* **11** 176–218
[121] Rosenthal D, McEachran R P and Cohen M 1974 *Proc. R. Soc. London* A **337** 365–78
[122] Guttmann A J and Wagenfeld H 1967 *Acta Crystallogr.* **22** 334–7
[123] Hildebrandt G, Stephenson J D and Wagenfeld H 1975 *Z. Naturf.* a **30** 697–707
[124] Bair R A and Goddard W A III 1980 *Phys. Rev.* B **22** 2767–76
[125] Müller J E and Wilkins J W 1984 *Phys. Rev.* B **29** 4331–48
[126] Matthew J A D, Netzer F P, Clark C W and Morar J F 1987 *Europhys. Lett.* **4** 677–83
[127] Liberman D and Zangwill A 1989 *Phys. Rev.* A **39** 415–6
[128] Sirotine Y and Chaskolskaïa M 1984 *Fondements de la Physique des Cristaux* (Moscow: Mir) pp 640–1
[129] Dräger G, Frahm R, Materlik G and Brümmer O 1988 *Phys. Status Solidi* b **146** 287–94
[130] Kosugi N, Yokoyama T, Asakura K and Kuroda H 1984 *Chem. Phys.* **91** 249–56
[131] Kosugi N, Yokoyama T and Kuroda H 1984 *EXAFS and Near Edge Structure III* ed. K O Hodgson, B Hedman and J E Penner-Hahn (Berlin: Springer) pp 55–7
[132] Yokoyama T, Kosugi N and Kuroda H 1986 *Chem. Phys.* **103** 101–9
[133] Kuiper P, Grioni M, Sawatzky G A, Mitzi D B, Kapitulnik A, Santaniello A, De Padova P and Thiry P 1989 *Physica* C **157** 260–2
[134] Hahn J E, Scott R A, Hodgson K O, Doniach S, Desjardins S R and Solomon E I 1982 *Chem. Phys. Lett.* **88** 595–8
[135] Stern E A, Sayers D E and Lytle F W 1976 *Phys. Rev. Lett.* **37** 298–301
[136] Kosugi N, Yokoyama T and Kuroda H 1986 *Chem. Phys.* **104** 449–53
[137] Kutzler F W, Scott R A, Berg J M, Hodgson K O, Doniach S, Cramer S P and Chang C H 1981 *J. Am. Chem. Soc.* **103** 6083–8
[138] Penner-Hahn J E and Hodgson K O 1986 *Structural Biological Applications of X-Ray Absorption, Scattering and Diffraction* ed. H D Bartunik and B Chance (Orlando, FL: Academic) pp 35–47
[139] Penner-Hahn J E, Smith T A, Hedman B, Hodgson K O and Doniach S 1986 *J. Physique Coll.* **47** C8 1197–200
[140] Penner-Hahn J E, Benfatto M, Hedman B, Takahashi T, Doniach S, Groves J T and Hodgson K O 1986 *Inorg. Chem.* **25** 2255–9

[141] Smith T A, Penner-Hahn J E, Berding M A, Doniach S and Hodgson K O 1985 *J. Am. Chem. Soc.* **107** 5945–55
[142] Tolentino H, Dartyge E, Fontaine A, Gourieux T, Krill G, Maurer M, Ravet M-F and Tourillon G 1989 *Proc. Int. Symp. on the Electronic Structure of High T_c Superconductors, 5–7 October 1988* (Oxford: Pergamon) pp 245–58
[143] Oyanagi H, Oka K, Unoki H, Nishihara Y, Murata K, Matsushita T, Tokumoto M and Kimura Y 1989 *Physica* B **158** 436–9
[144] Bianconi A, De Santis M, Di Cicco A, Flank A M, Fontaine A, Lagarde P, Katayama-Yoshida H, Kotani A and Marcelli A 1988 *Phys. Rev.* B **38** 7196–9
[145] Bianconi A, De Santis M, Flank A M, Fontaine A, Lagarde P, Marcelli A, Katayama-Yoshida H and Kotani A 1988 *Physica* C **153–155** 1760–1
[146] Tourillon G, Fontaine A, Garrett R, Sagurton M, Xu P and Williams G P 1987 *Phys. Rev.* B **35** 9863–6
[147] Tourillon G, Mahatsekake C, Andrieu C, Williams G P, Garrett R F and Braun W 1988 *Surf. Sci.* **201** 171–84
[148] Tourillon G, Garrett R, Lazarz N, Raynaud M, Reynaud C, Lécayon G and Viel P 1989 *J. Electrochem. Soc.* at press
[149] Stöhr J and Outka D A 1987 *Phys. Rev.* B **36** 7891–905
[150] Fernández Rico J and López R 1986 *J. Chem. Phys.* **85** 5890–4
[151] Kaufmann K and Baumeister W 1989 *J. Phys. B: At. Mol. Opt. Phys.* **22** 1–12
[152] Natoli C R 1983 *Springer Ser. Chem. Phys.* **27** 43–56
[153] Smith T A, Penner-Hahn J E, Hodgson K O, Berding M A and Doniach S 1984 *EXAFS and Near Edge Structure III* ed. K O Hodgson, B Hedman and J E Penner-Hahn (Berlin: Springer) pp 58–60
[154] Templeton D H and Templeton L K 1988 *J. Appl. Crystallogr.* **21** 151–3
[155] Weber W M 1979 *Phys. Status Solidi* b **91** 667–73
[156] Weber W M 1980 *Phys. Lett.* **78A** 51–3
[157] Stephens P J 1970 *J. Chem. Phys.* **52** 3489–516
[158] Werner E and Prantl W 1988 *J. Appl. Crystallogr.* **21** 311–6
[159] Tyliszczak T and Hitchcock A P 1989 *Physica* B **158** 335–6
[160] Sandstrom D R and Fine J M 1980 *Workshop on Laboratory EXAFS Facilities and their Relation to Synchrotron Radiation Sources, Seattle (WA) 28–30 April 1980, AIP Conf. Proc.* **64** 127–8
[161] Ponomarev Yu V and Turutin Tu A 1982 *Sov. Phys.–Tech. Phys.* **27** 129–30
[162] Hart M 1978 *Phil. Mag.* B **38** 41–56
[163] Starke W, Brümmer O, Dräger G, Nikiforov I Ya, Sachenko V P and Richter J 1972 *Bull. Acad. Sci. USSR, Phys. Ser.* **36** 219–22
[164] van der Laan G, Thole B T, Sawatzky G A, Goedkoop J B, Fuggle J C, Esteva J-M, Karnatak R, Remeika J P and Dabkowska H A 1986 *Phys. Rev.* B **34** 6529–31
[165] Schütz G, Wagner W, Wilhelm W, Kienle P, Zeller R, Frahm R and Materlik G 1987 *Phys. Rev. Lett.* **58** 737–40
[166] Stedman G E 1985 *Adv. Phys.* **34** 513–87
[167] Nye J 1957 *The Physical Properties of Crystals and their Representation by Tensors and Matrices* (Oxford: Oxford University Press) p 13
[168] Gaisenok V A 1988 *Opt. Spectrosc.* **64** 178–81
[169] Cornwell J F 1984 *Group Theory in Physics* vol I (London: Academic) p 258
[170] Gyorffy B L and Stott M J 1973 *Band Structure Spectroscopy of Metals and Alloys, University of Strathclyde, Proc. Int. Meeting on 26–30 September 1971* ed. D J Fabian and L M Watson (London: Academic) pp 385–403
[171] Durham P J 1988 *X-ray Absorption. Principles, Applications, Techniques of EXAFS, SEXAFS and XANES* ed. D C Koningsberger and R Prins (New York: Wiley) pp 53–84
[172] Stizza S, Benfatto M, Davoli I, Mancini G, Marcelli A, Bianconi A, Tomellini M and Garcia J 1985 *J. Physique Coll.* **47** C8 255–9
[173] Bianconi A 1984 *EXAFS and Near Edge Structure III* ed. K O Hodgson, B Hedman and J E Penner-Hahn (Berlin: Springer) pp 167–74
[174] Bianconi A, Congiu-Castellano A, Durham P J, Hasnain S S and Phillips S 1985 *Nature* **318** 685–7
[175] Berding M A 1985 *Stanford Synchrotron Radiation Laboratory Report* **85/04**
[176] Fujikawa T, Oizumi H, Oyanagi H, Tokumoto M and Kuroda H 1986 *J. Phys. Soc. Japan* **55** 4074–89
[177] Fujikawa T, Oizumi H, Oyanagi H, Tokumoto M and Kuroda H 1986 *J. Phys. Soc. Japan* **55** 4090–102
[178] Fujikawa T, Oizumi H, Oyanagi H, Tokumoto M, Ishiguro T and Kuroda H 1987 *Synth. Met.* **17** 75–80
[179] Fujikawa T, Tashiro K, Krone W and Kaindl G 1988 *J. Phys. Soc. Japan* **57** 320–8

[180] Penner-Hahn J E, Smith Eble K, Dawson J H, McMurry T J, Groves J T, Benfatto M, Doniach S, Hedman B and Hodgson K O 1987 *Biophysics and Synchrotron Radiation* (ed. A Bianconi and A Congiu Castellano (Berlin: Springer)
[181] Stöhr J, Outka D A, Baberschke K, Arvanitis D and Horsley J A 1987 *Phys. Rev.* B **36** 2976–9
[182] Morante S, Congiu-Castellano A, Dell'Ariccia M, Durham P J, Giovannelli A, Burrattini E and Bianconi A 1987 *Biophysics and Synchrotron Radiation* ed. A Bianconi and A Congiu Castellano (Berlin: Springer) pp 107–13
[183] Kitamura M, Sugiura C and Muramatsu S 1988 *Phys. Status Solidi* b **149** 791–7
[184] Kitamura M, Sugiura C and Muramatsu S 1988 *Solid State Commun.* **67** 313–6
[185] Tyson T A, Roe A L, Frank P, Hodgson K O and Hedman B 1989 *Phys. Rev.* B **39** 6305–15
[186] Tyson T A, Roe A L, Hedman B, Frank P and Hodgson K O 1989 *Physica* B **158** 398–9
[187] Garg K B, Bianconi A, Della Longa S, Clozza A, De Santis M and Marcelli A 1988 *Phys. Rev.* B **38** 244–51
[188] Maeyama S, Oshima M and Katsui A 1989 *Electr. Commun. Lab. Tech. J.* **38** 29–37
[189] Weber W M 1967 *Phys. Lett.* **25A** 590–1
[190] Wang Shengke, Waldo G S and Penner-Hahn J E 1989 *Physica* B **158** 253–4
[191] Fujimoto H 1966 *Sci. Rep. Tohoku Univ., Ser. 1* **49** 28–31
[192] Whitmore J, Ma Yanjun, Stern E A, Brown F C, Ingalls R L, Rice J P, Pazol B G and Ginsberg D M 1989 *Physica* B **158** 440–2
[193] Bianconi A, De Santis M, Di Cicco A, Flank A M and Lagarde P 1989 *Physica* B **158** 443–5
[194] Brümmer O and Dräger G 1966 *Phys. Status Solidi* **14** K175–9
[195] Wang Shengke, Waldo G S, Fronko R M and Penner-Hahn J E 1989 *Physica* B **158** 119–20
[196] Scott R A, Kazmi S A, Beinert H, Emptage M H, Hahn J E, Hodgson K O, Stout C D and Thomson A J 1983 *Inorg. Chim. Acta* **79** 142
[197] Weber W M 1962 *Physica* **28** 689–94
[198] Weber W M 1964 *Physica* **30** 2219–31
[199] Alexander E, Feller S, Fraenkel B S and Perel J 1965 *Nuovo Cimento* **35** 311–2
[200] Dräger G and Brümmer O 1984 *Proc. Int. Conf. on X-Ray and Inner-Shell Processes in Atoms, Molecules and Solids, Leipzig, 20–24 August 1984* ed. A Meisel and J Finster (Leipzig: Karl-Marx-Universität) pp 337–46
[201] George G N, Cleland W E Jr, Enemark J H, Kipke C A, Roberts S A and Cramer S P 1989 *Physica* B **158** 133–4
[202] Wong R, Roth W L, Dunn B and Yang D L 1986 *Solid State Ionics* **18–19** 599–602
[203] Takahashi T, Hayasi Y, Tokailin H, Asahina H, Morita A, Sagawa T and Shirotani I 1985 *Proc. 17th Int. Conf. on the Physics of Semiconductors, 6–10 August 1984, San Francisco* (New York: Springer) pp 1071–4
[204] Hayasi Y, Takahashi T, Asahina H, Sagawa T, Morita A and Shirotani I 1984 *Phys. Rev.* B **30** 1891–5
[205] Taniguchi M, Suga S, Seki M, Mikuni A, Asaoka S, Kanzaki H, Akahama Y, Endo S and Narita S 1984 *Phys. Rev.* B **30** 4555–63
[206] Tourillon G, Dartyge E, Palmans R and Frank A J 1989 *Physica* B **158** 208–10
[207] Watanabe M, Yamashita H, Nakai Y, Sato S and Onari S 1971 *Phys. Status Solidi* b **43** 631–6
[208] Levitski V M 1941 *Thesis* Gorki University (unpublished)
[209] Eldridge D C 1974 *PhD Thesis* Ohio University, Athens, USA
[210] Heald S M, Goldberg H A and Kalnin I L 1983 *Proc. Int. Conf. on EXAFS and Near Edge Structure, Frascati (Italy) 13–17 September 1982* ed. A Bianconi, L Incoccia and S Stipcich (Berlin: Springer) pp 141–3
[211] Stöhr J and Outka D A 1987 *J. Vac. Sci. Technol.* A **5** 919–26
[212] Rabe J P, Swalen J D, Outka D A and Stöhr J 1988 *Thin Solid Films* **159** 275–83
[213] Yang X Q, Chen J, Hale P D, Inagaki T, Skotheim T A, Okamoto Y, Samuelson L, Tripathy S, Hong K, Rubner M F and denBoer M L 1989 *Synth. Met.* **28** C251–6
[214] Himpsel F J, Karlsson U O, Morar J F, Rieger D and Yarmoff J A 1986 *Phys. Rev. Lett.* **56** 1497–500
[215] Oyanagi H, Yoneyama M, Ikegami K, Sugi M, Kuroda S, Ishiguro T and Matsushita T 1988 *Thin Solid Films* **159** 435–42
[216] Loupias G, Chomilier J, Tarbes J, Rabii S, Tatar R and Guérard D 1988 *Synth. Met.* **23** 205–10
[217] Yang X Q, Chen J, Hale P D, Inagaki T, Skotheim T A and denBoer M L 1989 *Synth. Met.* **28** C329–34
[218] Heald S M, Tranquada J M, Moodenbaugh A R and Xu Y 1988 *Mat. Res. Soc. Symp. Proc.* **99** 757–60
[219] Heald S M, Tranquada J M, Yang C Y, Xu Youwen, Moodenbaugh A R, Subramanian M A and Sleight A W 1989 *Physica* B **158** 433–5

[220] Penner-Hahn J E, Murata M, Hodgson K O and Freeman H C 1989 *Inorg. Chem.* **28** 1826–32
[221] Brümmer O and Dräger G 1966 *Röntgenspektren und chemische Bindung, Proc. Int. Symp. Leipzig, on 23–24 September 1965* ed. A Meisel (Leipzig: Karl-Marx-Universität) pp 35–43
[222] Schnopper H W 1966 *Röntgenspektren und chemische Bindung, Proc. Int. Symp. Leipzig, on 23–24 September 1965* ed. A Meisel (Leipzig: Karl-Marx-Universität) pp 303–13
[223] Schulz E 1986 *PhD Thesis* Martin Luther University, Halle-Wittenberg GDR (in German)
[224] Kosugi N, Kondoh H, Tajima H and Kuroda H 1989 *Physica* B **158** 450–2
[225] Della Longa S, Di Cicco A, Stizza S, De Santis M, Garg K and Bianconi A 1989 *Physica* B **158** 469–70
[226] Alp E Ercan, Mini S M, Ramanathan M, Veal B W, Soderholm L, Goodman G L, Dabrowski B, Shenoy G K, Guo J, Ellis D E, Bommanavar A and Hyun O B 1989 *Mat. Res. Soc. Symp. Proc.* **143** 97–102
[227] Yakushi K, Yamakado H, Yoishitake M, Kosugi N, Kuroda H, Sugano T, Kinoshita M, Kawamoto A and Tanaka J 1989 *Bull. Chem. Soc. Japan* **62** 687–96